Variability of single event slip and recurrence intervals for large magnitude paleoearthquakes on New Zealand's active faults

A. Nicol
R. J. Van Dissen
R. Robinson
A. Harvison

GNS Science Report 2012/41
December 2012

GNS SCIENCE
TE PŪ AO

Variability of single event slip and recurrence intervals for large magnitude paleoearthquakes on New Zealand's active faults

A. Nicol
R. J. Van Dissen
R. Robinson
A. Harvison

GNS Science Report 2012/41
December 2012

BIBLIOGRAPHIC REFERENCE

Nicol, A.; Robinson, R.; Van Dissen, R. J.; Harvison, A. 2012. Variability of single event slip and recurrence intervals for large magnitude paleoearthquakes on New Zealand's active faults, *GNS Science Report* 2012/41. 57 p.

A. Nicol, GNS Science, PO Box 30368, Lower Hutt 5040, New Zealand
R. Robinson, PO Box 30368, Lower Hutt 5040, New Zealand
R. J. Van Dissen, PO Box 30368, Lower Hutt 5040, New Zealand
A. Harvison, PO Box 30368, Lower Hutt 5040, New Zealand

ISSN 1177-2425
ISBN 978-1-972192-29-0

CONTENTS

FIGURES

TABLES

APPENDICES

LAYMANS ABSTRACT

The time between success prehistoric earthquakes (referred to here as recurrence interval) and their slip at the ground surface during these events can vary significantly through time. Understanding these variations is important for estimating the likelihood of future hazardous earthquakes on active faults in New Zealand. To improve our knowledge of variations in earthquake recurrence intervals and slip we have gathered existing (published and unpublished) geological information and synthetic earthquakes generated by numerical models for over 100 of New Zealand's active faults. Synthetic earthquakes help fill information gaps in the natural (geological) data which may arise due to measurement uncertainty and to the brevity of the geological record (i.e. < 30 thousand years and <10 surface-rupturing earthquakes on each fault). For prehistoric earthquakes recurrence intervals can be highly variable, often being less than the average and occasionally up to four times the average. Recurrence intervals for synthetic earthquakes show less variability between faults than the geological data, which may be partly due to the significantly larger number of events in the synthetic record. For prehistoric earthquakes slip on individual active faults appears to be less variable than recurrence interval. This difference in variation has been quantified for each fault using a statistical measure referred to as the Coefficient of Variation (COV=standard deviation divided by the average). Coefficients of Variation of 0.4±0.2 and 0.6±0.25 have been proposed for earthquake slip and recurrence interval, respectively. These Coefficients of Variation only apply to the largest earthquakes that ruptured the ground surface and are routinely observed in the geological record. For the purposes of this report the prehistoric earthquake record of the best studied faults is assumed to be complete for magnitudes of ≥7.2±0.2 and ≥6.1±0.2 for strike slip faults and normal faults, respectively. More data and analysis are required however to quantify the completeness of the geological data and to understand better how this may be impacting our results. Despite these outstanding questions, our results for recurrence interval and single event slip provide constraints on the variability of these parameters and could be applied to active faults in the NSHM for which there are insufficient data to constrain their prehistoric history.

TECHNICAL ABSTRACT

Recurrence intervals and single event slip for large magnitude earthquakes that ruptured the ground surface can vary by more than an order of magnitude on individual faults. To quantify this variability we combine existing (published and unpublished) geological observations and synthetic earthquakes generated by numerical models for over 100 of New Zealand's active faults. Synthetic earthquakes generated for fault systems help fill information gaps in the natural (geological) data which may arise due to measurement uncertainty and to the brevity of the geological record (i.e. <10 surface-rupturing earthquakes per fault). These datasets define frequency histograms and probability density functions (PDFs) for recurrence interval and single event slip. They are also used to determine the coefficient of variation (COV) for recurrence interval and single event slip. Although the shapes of histograms generated from geological data using a Monte Carlo method are variable, recurrence intervals for the best data (i.e. ≥7 surface-rupturing events) are often asymmetric with modes less than, or equal to, the mean and a long recurrence (3-4 times the mean) tail. The resulting PDFs for recurrence interval more closely resemble log-normal or Weibull than normal distributions, in contrast to the single event slip for geological data and synthetic models which in many cases are approximately normal. Recurrence interval histograms for synthetic earthquakes show less variability between faults than the geological data, which may be partly due to the significantly larger number of events in the synthetic dataset. Histograms and PDFs for recurrence intervals of synthetic earthquakes are similar to the geological data in that they exhibit a long recurrence interval tail which constitutes a small proportion (<20%) of the total population. COV for recurrence interval (0.58±0.2 geological and 0.56±0.27 synthetic) and single event slip (0.4±0.2 geological) suggest that recurrence is more variable than single event slip. COV for single event slip (0.4±0.2) and recurrence interval (0.6±0.25) are inferred to have a minimum magnitude of completeness (Mc) for geological data of 7.2±0.2 and 6.1±0.2 for strike slip faults and normal faults, respectively. More data and analysis are required however to quantify the Mc for geological data and to understand better how this may be impacting on the geological and synthetic results. In addition, more research is required to define better the PDFs for recurrence interval and single event slip before these can be input into the New Zealand National Seismic Hazard Model (NSHM). Despite these outstanding questions, COV for recurrence interval and single event slip provide constraints on the variability of these parameters and could be applied to active faults in the NSHM for which there are insufficient data to constrain their paleoearthquake history.

KEYWORDS

Single event slip, recurrence interval, paleoearthquakes, synthetic seismicity, minimum completeness magnitude

1.0 INTRODUCTION

Large magnitude earthquakes pose major hazards in plate boundary regions, such as New Zealand. Forecasting when and where these earthquakes will occur has proven problematic in part because, for individual faults, their recurrence intervals (i.e. time between events) and sizes (i.e. single event slip) can vary by an order of magnitude or more (e.g., Wallace, 1987; McCalpin and Nishenko, 1996; Marco et al., 1996; Dawson et al., 2003; Friedrich et al., 2003; Palumbo et al., 2004; Weldon et al., 2004; Mouslopoulou et al., 2009a). These geological observations, which have been confirmed by million-year synthetic seismicity models of fault systems (Robinson, 2004; Robinson et al., 2009a, 2009b, 2011), indicate that earthquake parameters are sufficiently variable to warrant inclusion of this variability in earthquake hazard models. In this report the variability of recurrence and single event slip has been quantified using natural (geological) and synthetic surface-rupturing earthquakes on over 100 New Zealand active faults. These data include 27 active faults for which the timing and/or single event slip are available from geological observations. The results are presented in such a way that they can be incorporated into future versions of the New Zealand National Seismic Hazard Model (NSHM) (e.g., Stirling et al., 2002 & 2012), to help improve forecasting of earthquake hazard.

Many processes could contribute to variability of earthquake parameters, including temporal changes of fault strength, fault segmentation, fault healing rate, fault loading rate and fault interactions (e.g., Wallace, 1987; Weldon et al., 2004; Nicol et al., 2009). The present study focuses on quantifying the variability rather than examining the underlying processes. It utilises a large quantity of published and unpublished geological data on the timing and slip of paleoearthquakes amassed in New Zealand, particularly over the last 10 years. The faults for which geological data are available are listed in Table 2.1 while their locations are shown on Figure 2.1 and earthquake histories tabulated in Appendix 1. Geological data are complemented by large magnitude earthquakes generated by synthetic seismicity models for active fault systems in the Wellington, Marlborough and Bay of Plenty regions of New Zealand (including 12 of the faults in Table 2.1) (Robinson, 2004; Robinson et al., 2009a, 2009b, 2011). Synthetic earthquakes help fill information gaps in the geological data which may arise due to measurement uncertainty and to the brevity of the geological record (i.e. <10 surface-rupturing earthquakes per fault). Together geological and synthetic earthquakes provide a large dataset for estimating the variability of recurrence interval and single event slip. In this report presentation of the data (i.e. sources and sampling issues) and methods of analysis are augmented by discussion of the natural and synthetic surface-rupturing earthquake recurrence and single event slip for a range of fault types, slip rates and dimensions. These datasets are used to develop frequency histograms and probability density functions (PDFs) for recurrence interval and single event slip. They have also been used to define the coefficient of variation (COV) for recurrence interval and single event slip. Generic COVs for recurrence interval and single event slip have the potential to be applied to active faults in the NSHM for which there are insufficient data to constrain the paleoearthquake history. The results of this work are preliminary and more research is required to improve definition of the PDFs for recurrence interval and single event slip.

2.0 GEOLOGICAL EARTHQUAKES

2.1 DATA SOURCES

Active fault traces in New Zealand with a topographic expression are produced by surface-rupturing earthquakes. Over the last 30 years, analysis of fault trench logs and displacement of dated landforms has generated a large body of data on the paleoearthquake histories of these active faults (e.g., see references in Table 2.1). These datasets provide evidence of progressive displacement and deformation of dated near-surface stratigraphy or geomorphic surfaces which enable the timing and/or slip during past earthquakes to be estimated (for discussion of methods see McCalpin, 1996). These paleoearthquake data provide information for <10 surface-rupturing earthquakes on individual faults in New Zealand over time intervals of up to about 30 thousand years (Table 2.1). For the purposes of this study we utilise published and unpublished information for faults on which four or more past earthquakes have been recorded. Table 2.1 lists the 27 faults that satisfy this criterion and for which their paleoearthquake histories have been analysed. Paleoearthquake histories from the published literature have been accepted as is, except where these papers are augmented by later work (either published or unpublished), in which case we have generated earthquake histories that are consistent with all of the available data. In some instances we have elected not to accept the proposed timing of prehistoric earthquakes because the inferences previously presented have been superseded by new data. For example, along the eastern onshore section of the Wairau Fault the proposed post 1000 AD timing of the last event (Grapes and Wellman, 1986; Yetton, 2003) has been rejected here as new unpublished radiocarbon dating suggests that this event occurred about 2000 years ago (Van Dissen and Nicol, unpublished data 2012). The number of prehistoric events for which recurrence intervals were estimated varies between faults from 4 to 9, while the record of single event slip is generally less complete. In about two-thirds of cases, for example, estimates of the single event slip are only available for the last one or two surface-rupturing events.

Table 2.1 Summary of faults and paleoearthquake information from geological datasets in this study. Timing of events and recurrence rounded to nearest 10 years. Single event slip (and uncertainty) rounded to nearest 10 cm. See Appendix 1 for raw paleoearthquake data and Figure 2.1 for fault locations. † Slip rates calculated for approximately the duration of the paleoearthquake record. In single event slip column "*" denotes mean calculated for two or three events only. Alpine Fault data excludes Hokuri Creek data of Berryman et al. (2012) as these were not available at the time of analysis.

	Fault	Fault type	Slip rate†		Number of EQs	Recurrence (yrs)		Single event slip (m)		Synthetic	Oldest event		Last event		Ratio sample interval to mean recurrence	Data source
			(mm/yr)	Error (2σ)		Mean	Std. Dev.	Mean	Std. Dev.	seismicity model	yrs before 2010	Error (2σ)	yrs before 2010	Error (2σ)		
1	**Eastern Awatere**	SS	6	2	9	930	540	5.2*	0.2	Y	8530	140	162	0	9.17	Benson et al. 2001, Mason et al. 2006
2	**Rotoitipakau**	N	1.7	0.1	9	1315	1130			N	10560	1000	23	0	8.02	Berryman et al. 1998
3	**Wairau**	SS	3.2	0.5	9	2260	1340	7.7	2.4	Y	17960	2300	2000	100	7.91	Zacharison et al. 2006, Barnes & Pondard 2010, Van Dissen and Nicol unpublished data, 2012
4	**Rangipo**	N	0.23	0.03	8	1890	1570	0.5*	0.4	N	12110	250	1010	250	6.29	Villamor et al. 2007
5	**Whirinaki**	N	0.7	0.3	8	3360	2050	0.9	0.4	Y	24060	3000	560	50	7.17	Canora-Catalán et al. 2008
6	**Paeroa**	N	1.6	0.2	7	2620	1990	1.8	1.0	Y	16200	800	460	140	6.18	Berryman et a. 2008
7	**Pihama**	N	0.1	0.05	7	10660	8180	0.9	0.4	N	67060	12500	3060	3000	6.29	Townsend et al. 2010, Mouslopoulou et al. 2012, Nicol et al., unpublished data 2011
8	**Cloudy**	SS?	2.5	1.5	6	3000	2120	2.9	1.8	N	16200	3700	1800	300	5.63	Pondard & Barnes 2010
9	**Mangatete**	N	0.5	0.1	6	4640	1480	1	0.4	N	24210	2350	1010	750	5.22	Nicol et al., 2007, Nicol et al. unpublished data 2011
10	**Eastern Porters Pass**	SS	3.6	0.5	6	1630	960	6.3	1.2	N	8760	300	610	50	5.37	Howard et al. 2005
11	**Southern Wairarapa**	SS/R	11	3	6	1330	360	16.9*	3.4	Y	6825	155	155	0	5.12	Rodgers & Little 2006, Little et al. 2009
12	**Alpine**	SS	23	2	5	149	47	8.5*	0.5	Y	780	50	184	25	5.32	Wells et al. 1999, Wells & Goff 2007, Yetton & Wells 2010
13	**Hope (Hope Segment)**	SS	11	0.5	5	130	30			Y	630	34	122	0	4.96	Cowan & McGlone 1991
14	**Kiri**	N	1.4	0.3	5	910	710			N	4560	1500	990	770	5.11	Townsend et al. 2010, Mouslopoulou et al. 2012, Nicol et al., unpublished data 2011
15	**Lachlan**	R	4.5	1.5	5	1180	620			N	5343	75	610	100	4.52	Berryman 1993, Barnes et al. 2002
16	**Ngakuru**	N	0.5	0.1	5	8540	5380	1.4	0.6	Y	26320	920	690	300	3.08	Nicol et al. unpublished data 2011
17	**Ohariu**	SS	1.5	0.5	5	1180	460			Y	4900	500	205	55	4.17	Heron et al. 1998, Litchfield et al. 2006, Litchfield et al. 2010
18	**Snowdon**	N	0.2	0.1	5	4760	2710	0.5	0.2	N	20060	2500	1010	750	4.21	Nicol et al. 2007, Nicol et al. unpublished data 2011
19	**Vernon**	SS	3	2	5	3140	1890	1.2	0.8	N	15300	3500	3200	700	5.06	Pondard & Barnes 2010
20	**Wellington (Hutt Valley)**	SS	6.1	2	5	1910	1440	5.0	1.5	Y	7895	545	270	545	4.14	Little et al., 2010, Langridge et al., 2011
21	**Eastern Clarence**	SS	4	1	4	1590	920	7.0*	2	Y	6600	400	1820	160	4.14	Van Dissen & Nicol 2009
22	**Ihaia**	N	0.35	0.15	4	1820	680			N	5860	500	410	200	3.23	Mouslopoulou et al. unpublished data 2011, Mouslopoulou et al. 2012
23	**Matata**	N	4.1	1.5	4	790	490			N	2560	800	270	50	3.35	Ota et al. 1988, Begg & Mouslopoulou 2010
24	**Oaonui**	N	0.11	0.04	4	7620	2770	0.5	0.1	N	23800	1200	990	720	3.13	Townsend et al. 2010
25	**Rotohauhau**	N	0.6	0.1	4	5100	4870	0.8	0.2	Y	16360	900	1010	750	3.20	Nicol et al. 2007, Nicol et al. unpublished data 2011
26	**Waimana**	SS/N	1.2	0.7	4	2910	940			N	11060	1500	2310	450	3.80	Mouslopoulou 2006, Mouslopoulou et al. 2009b
27	**Whakatane**	SS/N	2	1	4	2450	1970			N	8800	700	1460	700	3.60	Mouslopoulou 2006, Mouslopoulou et al. 2009b

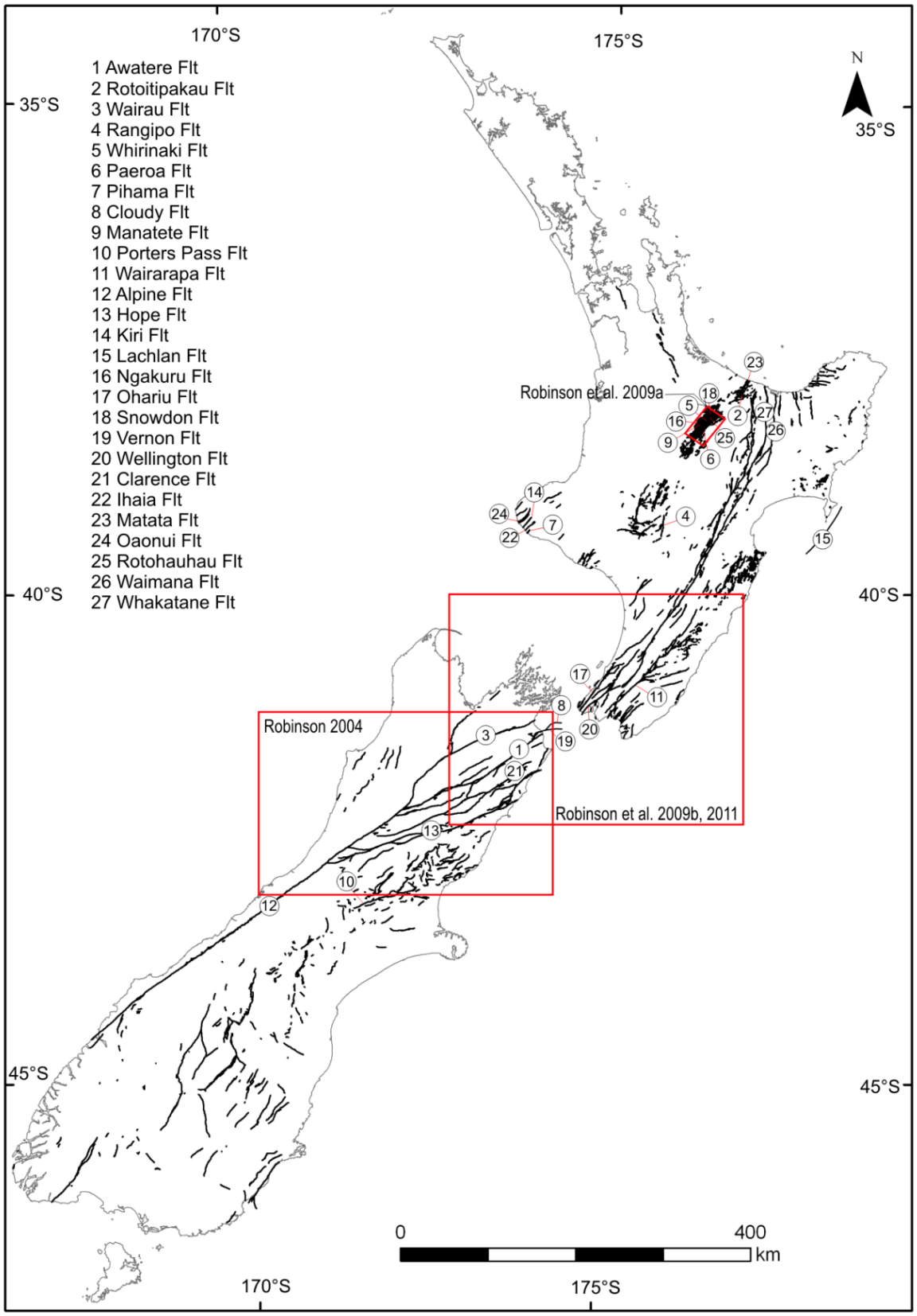

Figure 2.1 Active fault map of New Zealand showing the locations of faults (thick black lines) listed in Table 2.1. Fault numbers correspond to those given in the left-hand column of Table 2.1. Fault locations form the GNS Science active faults database (GNS open access, August 2012). Red boxes show regions of synthetic seismicity models.

As with most paleoearthquake studies globally, geological estimates of the timing and slip of events in New Zealand include some uncertainty. These uncertainties generally increase with the age of the earthquake and with the number of subsequent events. They also increase with a decrease in the number of observations constraining the timing and slip during a particular earthquake. Uncertainties on average single event slip and earthquake timing are generally ≤~±40% and are often subjectively considered (i.e. without statistical analysis) to present the 95% confidence level (e.g., Van Dissen and Nicol, 2009; Little et al., 2010). This use of the 95% confidence limit is intended to indicate that we believe that the uncertainty range is highly likely to contain the true value but that there is a small chance it does not. Uncertainties for paleoearthquakes are adopted from source documentation or, where there are multiple documents, revised so that they are consistent with all of the available high-quality data. Uncertainties for all paleoearthquakes analysed in this study are presented in Appendix 1.

2.2 SAMPLING ARTEFACTS

In addition to these uncertainties the estimated recurrence intervals and single event slip could be influenced by a number of sampling artefacts which, like the uncertainties, impact on all studies using paleoseismic data. These artefacts are discussed briefly below and mainly arise either because most paleoseismic data are from one-dimensional samples (i.e. point sources or single locations along a surface trace) on a three-dimensional active fault surface or due to the fact that not all earthquakes on a fault produce rupture (and associated displacement) at the ground surface that can be resolved using the techniques currently available (e.g., trenching, geomorphic analysis and shallow seismic reflection lines).

Some variability in recurrence intervals and single event slip could arise because paleoearthquake data are typically one-dimensional samples on traces along which earthquake slip typically varies (e.g., Hemphill-Haley and Weldon, 1999; Biasi and Weldon, 2006; Wesnousky, 2008; Nicol et al., 2010). Point sampling may impact on measurements of paleoearthquake parameters because; i) each earthquake may not rupture the entire length of a fault trace, ii) single event slip may vary along a trace for an individual earthquake (e.g., Figure 2.2), and iii) changes in slip distributions along fault traces occur between earthquakes. These issues are most extreme on long faults and approaching fault tips where single event slip is likely to be lower than elsewhere on the fault. For example, along the Alpine Fault in New Zealand, which is at least 500 km long, the average recurrence interval at a point towards the southern end of the fault trace is ~330 years for 8000 years (Berryman et al., 2012), while the average recurrence for the entire fault over the last 500 years was ~150-160 years (Wells et al., 1999; Wells and Goff, 2007; Yetton and Wells, 2010). This factor of two difference may arise due to a number of factors including, a change from one to two dimensional sampling arising because not all earthquakes rupture the entire fault (e.g., the southern end of the fault) which could have implications for the variability of earthquake parameters. Similarly, point samples close to fault tips have the potential to miss events (overestimate the recurrence interval) or significantly underestimate the maximum or mean single event slip (Figure 2.2). Much of our data is derived from the central sections of faults and may not be subject to near-tip sampling problems. A solution to point sampling issues would be to determine the timing of paleoearthquakes and their slip at multiple points along each active fault. At present such two-dimensional sampling of paleoearthquakes has not been widely conducted on New Zealand's active faults, but is expected to be become increasingly common in future as more data are collected. Because of the lack of widespread two-dimensional geological data we have chosen to test the results from geological data by comparing them to synthetic earthquakes for the same faults and for which the impact of one

dimensional sampling can be assessed. Our underlying philosophy is that if the first-order observations from both geological and synthetic datasets are comparable, then it is possible that the resulting conclusions are not significantly impacted by sampling issues or by model setup and implementation (e.g., physical approximations).

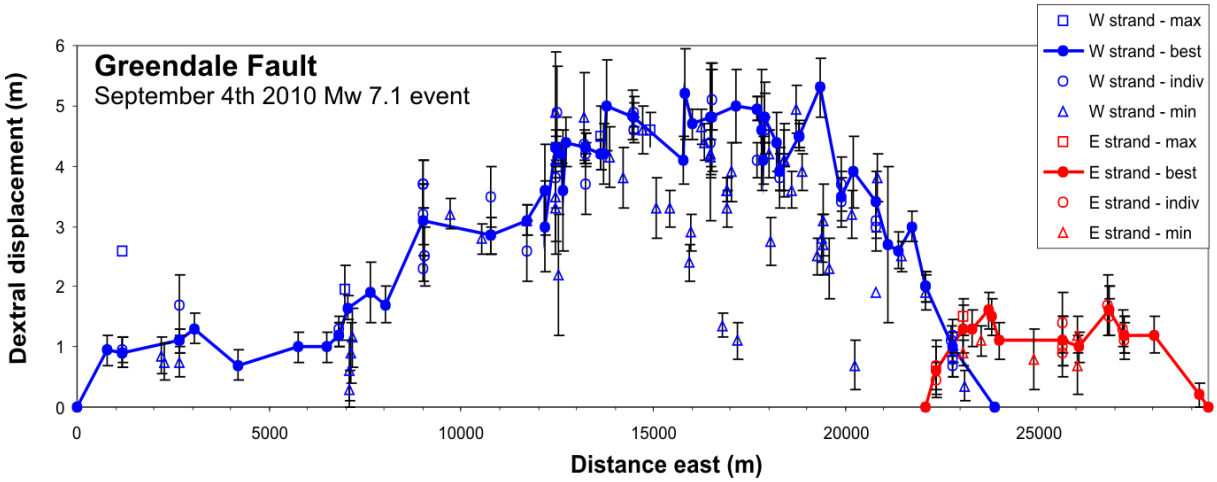

Figure 2.2 Displacement profile along the surface rupture of the Greendale Fault 2010 Mw 7.1 Darfield earthquake (modified from Quigley et al., 2012). Blue and red lines show displacement variations using the 'best' measurements for the west (W) and east (E) fault strands, respectively. The different types of measurement are: max, maximum of multiple measurements; best, preferred measurement from multiple measurement; indiv, one measurement; min, minimum of multiple measurements.

A second important limitation of the geological data is that not all paleoearthquakes on an active fault will be resolvable at, or near, the ground surface. This lack of resolution could arise because these events did not rupture the ground surface or because surface erosion or deposition processes are sufficiently fast to remove or conceal evidence of a particular earthquake. One consequence of this incompleteness is that the number of active faults and potential earthquake sources may be significantly higher than has been observed (Wells and Coppersmith, 1993; Lettis et al., 1997; Nicol et al., 2011a). In the Taranaki Rift southwest of Mt Taranaki (i.e. location of faults 7, 22 & 24 in Figure 2.1 and Table 2.1), for example, seismic reflection lines reveal that ≤ 50% of potential active faults have resolvable surface traces (Mouslopoulou et al., 2012). Quantifying this sampling limitation and estimating its impact on the geological data can be undertaken by considering the size of earthquake (e.g., slip and magnitude) we could reasonably expect to be routinely resolved in the geological data and by using the historical earthquake catalogue to determine what earthquake magnitudes resulted in surface rupture. In the former case the minimum slip we would expect to see can be estimated and used to infer the minimum expected event magnitude for a given fault. This minimum will vary between faults and is dependent on many factors including, the type of fault (strike slip, normal or reverse) and the rates and types of surface processes. For many of New Zealand's strike slip faults recording single event slip less than 3 m will be difficult and, using the maximum displacement magnitude regression of Wells and Coppersmith (1994) for strike slip faults, would suggest that slip information is unlikely to be available for all events ≤M7.2.

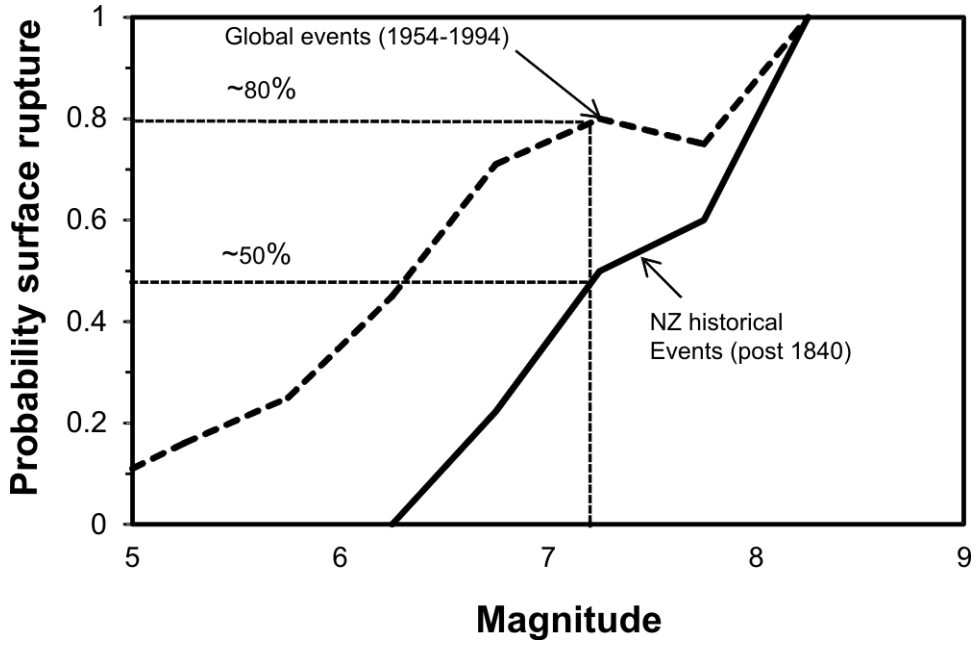

Figure 2.3 Probability of surface rupture for earthquakes beneath the New Zealand landmass since 1840 (solid line) (data from Downes, in press) and from the Wells and Coppersmith (1994) global compilation of historical earthquakes from 1954-1994 (dashed line).

An indication of the magnitude of events that are unlikely to rupture the ground surface is provided by Figure 2.3. Here we have plotted the probability of surface rupture against magnitude for historical shallow crustal (<30 km depth) NZ events post 1840 and global earthquakes from Wells and Coppersmith (1994). Because earthquakes recorded prior to the routine use of instrumental data could be biased towards surface rupturing events (e.g., Wells and Coppersmith, 1993) we have elected to use events in the global database from 1954-94. Both datasets show a decrease in the probability of events rupturing the ground surface with decreasing magnitude; the global curve being similar to that presented by Lettis et al. (1997) and Wells & Coppersmith (1993) (Figure 2.3). Fewer historical New Zealand earthquakes appear to have ruptured the ground surface for a given magnitude (e.g., 50% vs 80% for M7.2) than global events from which it could be concluded that surface ruptures were under recorded in New Zealand (this may have been of particular importance in the 19th century). Irrespective of the cause(s) of the discrepancy between the two datasets it seems that no more than one third and three quarters of magnitude 6 and 7 events rupture the ground surface respectively. These proportions may vary between different fault types and could have two important implications for the observed earthquake parameters from geological data. First, geological data typically only sample those large magnitude events that rupture the ground surface (e.g., > M6-7), therefore they will tend to indicate that these large events are quasi-Characteristic (i.e. they will have a similar magnitude and single event slip, see Schwartz and Coppersmith, 1984). We suggest that because of this completeness issue caution should be exercised when attempting to use geological paleoearthquake data to differentiate between Characteristic and Gutenberg-Richter earthquake models for individual faults (e.g., Schwartz and Coppersmith, 1984; Wesnousky, 1994). Second, because some events on each fault will not be recorded by a geological sample these data should be regarded as maximums for the average recurrence interval and the average single event slip. There are currently insufficient data to assess how many events have been missed on New Zealand faults. One potential means of addressing this issue is to adopt the minimum magnitude of completeness (Mc) concept widely used in seismology (e.g., Wiemer and Wyss, 2000), where Mc would be the magnitude down to (and including) which all earthquakes on a fault were sampled by the geological data. We suggest that recurrence

interval and single event slip for all paleoearthquake data should be quoted with a magnitude of completeness, however, we concede that estimating Mc may not be trivial in some cases. One approach to assigning an Mc would be to estimate the minimum slip that could be routinely observed in the geological record. For normal faults in the Taupo Rift southeast of Rotorua, for example, it may be possible to routinely record single event slip as small as ~0.2 m which, using displacement-moment magnitude regressions from Wells and Coppersmith (1994), would suggest an Mc of ~6.1.

Incompleteness of geological paleoearthquakes must be estimated before comparing natural and synthetic datasets for the same faults. To facilitate this comparison the synthetic earthquake catalogue should be sub-sampled so that it only includes events with magnitudes at the geological Mc or above. For the purposes of this report Mc has been estimated for synthetic earthquakes by assuming that Characteristic events in frequency-magnitude plots would be observed at the ground surface in geological datasets. Using this criterion Mc for reverse and strike slip faults typically range from M 7.0 to 7.4 (i.e. 7.2±0.2) and for normal faults from M5.9 to 6.3 (6.1±0.2) (Robinson et al., 2009a, 2009b, 2011). These estimates are consistent with our Mc estimates of 6.1 and 7.2 for geologically recordable displacements of normal and strike slip faults, respectively. These estimates of Mc for geological and synthetic earthquake data are considered first-order only as, for example, they do not take account of any variability between faults or differences between the sample dimensionality of geological (point measurements) and synthetic (fault trace or surface measurements) earthquakes. We note, however, that Mc adjusted synthetic datasets for 1-D (point samples) and 2-D (fault trace measurement) samples from the Wairau Fault do not significantly change the histogram location or shape for recurrence intervals on this structure.

While our analysis to date suggest that the Mc values used may be approximately correct, further refinement of these estimates may be possible and will form the focus of future work.

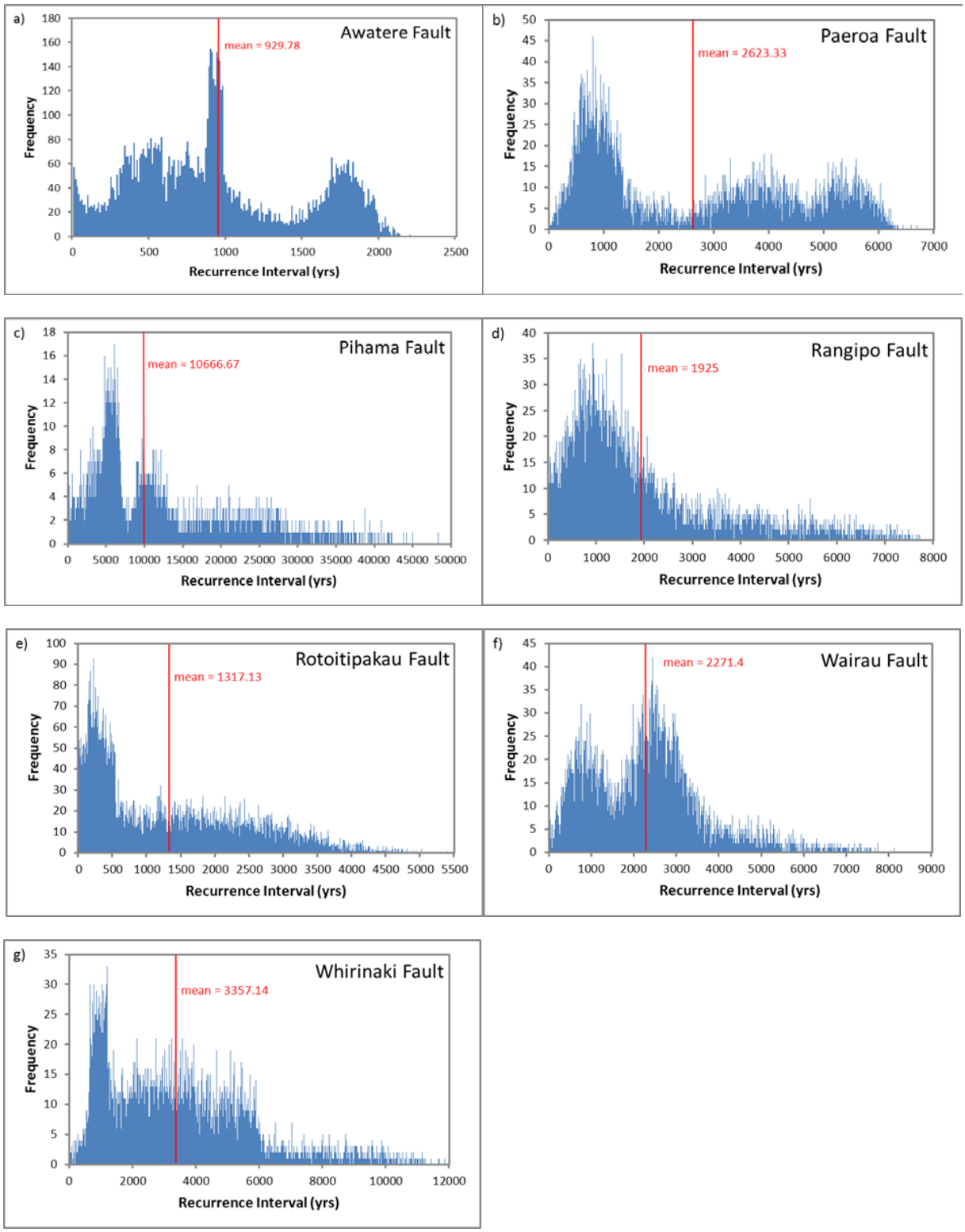

Figure 2.4 Recurrence interval histograms for individual active faults with 7 or more recorded surface-rupturing earthquakes generated using the data in Appendix 1 and the Monte Carlo method outlined in the "Data Analysis" section.

3.0 SYNTHETIC EARTHQUAKES

Synthetic seismicity models have been developed for fault systems in three regions in New Zealand (see Figure 2.1 for locations). Dislocation modelling of large magnitude earthquakes within fault systems permits the size and recurrence intervals of these events to be determined over time intervals of millions of years (e.g., Ben-Zion, 1996; Ward, 2000; Fitzenz and Miller, 2001; Rundle et al., 2006). The strength of these synthetic earthquake models is that they can be designed to replicate the regional tectonics, slip rates and geometries of real fault systems and produce data for hundreds (and in some cases thousands) of large magnitude earthquakes on each fault. Our computer generated seismicity catalogue provides a long (in excess of 1 million years) and complete record for more than 100 of New Zealand's active faults. The long duration of the synthetic models was selected to provide statistically meaningful seismicity datasets and is not intended to convey the view that the present geometries, kinematics and earthquake histories of active faults apply for millions of years. Analysis of these synthetic earthquakes suggests that, like earthquakes on natural faults, they are characterised by variations in single event slip and recurrence intervals (Robinson, 2004; Robinson et al., 2009a, 2009b, 2011).

The synthetic seismicity models replicate static stress build-up during tectonic loading with fault failure and earthquake rupture when the fault strength is exceeded (Robinson and Benites, 1996, 2001; Robinson, 2004). These models have been developed for parts of the Bay of Plenty, Wellington and Marlborough regions of New Zealand and consist of five key elements: 1) A geometric description of the natural faults in the region of study, which are finely divided into small cells (e.g., as small as 200 x 200 m); 2) frictional behaviour defined by a variable coefficient of friction and of static/dynamic type, with healing; 3) a driving mechanism that loads the faults toward failure; 4) fault failure based on the Coulomb Failure Criterion; and 5) fault interactions via induced changes in static stress and pore pressure. The driving mechanism results in the initial failure of one fault cell that in turn induces changes in stress/pore pressure on all other cells, on all faults. If loaded sufficiently, other cells then fail as part of the same event, and so on. The more cells that slip during a failure event the larger the magnitude of the synthetic earthquake. Thus, once the initial conditions of the model have been specified, it is deterministic, not stochastic. The formulation of Okada (1992) for a uniform elastic half-space is used to calculate the induced fault displacements and their spatial derivatives, and hence stresses. Induced stresses propagate through the medium at the shear-wave velocity and all faults in each model interact elastically. The model rigidity is 4.0×10^{10} Nm-2 and the density is 2.65×10^{3} kgm^{-3}, which are reasonable first approximations for the brittle crust in New Zealand (Robinson and Benites, 1996, 2001). Parameters of the model are adjusted to reproduce the geologically observed long-term (> ~10 kyr) displacement rates and a regional b-value of ~1.0. These properties together with earthquake single event slip and recurrence intervals emerge from the model and are dependent on its geometry, dynamics and rheology.

The synthetic seismicity catalogues used in this study were generated over about 15 years commencing in 1997 and have been analysed in a number of publications (Robinson, 2004; Robinson et al., 2009a, 2009b, 2011). The resulting earthquakes have been generated for a total of 119 primary normal and strike-slip faults (i.e. faults that have been recognised by geological mapping), with slip rates of ~0.1 to 25 mm/yr together with ~10 000 randomly distributed additional small faults (i.e. 1-2.5 km in length). The result is a long catalogue of about five million events with magnitudes of M~4 to 8.1, which simulate a time period of up to 2 million years. The earthquake populations produced by this type of model have been

shown to reproduce earthquake magnitudes and recurrence intervals typical of natural faults (Somerville et al., 1999; Robinson and Benites, 2001). Our comparisons (between geological and synthetic data) in this report confirm this conclusion and suggest that synthetic earthquakes approximately replicate the general form and variability of size and recurrence interval for geologically determined earthquakes. Thus, output from existing synthetic earthquake models and from geological paleoearthquake studies has been combined to quantify the variability of earthquake recurrence intervals and single event slip.

4.0 DATA ANALYSIS

Variability of recurrence interval and single event slip has been assessed for paleoearthquake data using a combination of frequency histograms, probability density functions (PDF) and the Coefficient of Variation (COV=Standard deviation/arithmetic mean) for recurrence interval and single event slip. Frequency histograms of recurrence interval and single event slip were generated for some of the faults in Table 2.1 using a Monte Carlo method together with the earthquake parameters and uncertainties presented in Appendix 1.

The Monte Carlo procedure, similar that previous employed by others (e.g., Parsons, 2008), has been used to generate frequency histograms for faults using natural earthquake input data and is described below. First a PDF was assigned to the timing and single event slip for each event identified in the geological record. The uncertainty bounds for the underpinning data are assumed to represent the 95% confidence limit for each PDF, with the probability distribution between the 95% limits being unknown, which is typically true for event timing. For the purposes of this study we selected a PDF which was evenly distributed about the mean with events in the central 95% of the distribution having equal probability. The central 95% was bounded by two 2.5% tails decreasing in probability with increasing distance from the mean (the decay was equivalent to that of a normal distribution). This PDF was applied to all events on all faults, however, it remains possible that each event had a different PDF or that all faults have approximately the same PDF which is different to our standard model. To test the second of these possibilities we also used a normal distribution with the same 95% confidence limits as the standard model and a uniform probability model where the uncertainty bounds are equal to the 100% confidence limits. Neither of these alternate models produced significantly different results or conclusions to the standard model. Here we only present output for the standard model.

The timing and slip for each event were drawn randomly from the PDFs for each parameter (recurrence and slip) commencing with the youngest earthquake. Preceding (older) events randomly drawn from their PDFs were retained if they produced a positive recurrence interval (i.e. Recurrence interval = oldest event – youngest event). If the timing of the older event produced a zero or negative recurrence interval the value for the older event was discarded and a new age for the older event randomly sampled from the PDF until a positive value was attained. This process is repeated until a Monte Carlo slip and timing estimate had been assigned for each earthquake observed in the geological database. One thousand paleoearthquake histories (i.e. modelling all geologically recognised events on each fault) were generated for all faults in Table 2.1. The resulting stochastic output has been plotted as histograms for recurrence (e.g., Figure 2.4) and single event slip. The Monte Carlo generation of histograms was undertaken multiple times (e.g., 2-10) for the same fault. Comparison of the histograms for different runs confirmed that their general shapes did not change significantly between runs. Given this stability we present a single model output for each fault.

The histograms take account of the average timing and slip of events and also reflect the uncertainties in these values. They have been used to generate PDFs (e.g., Figure 4.1) for faults with ≥7 events in Table 2.1 by dividing the frequencies in each 10 year bin by the total number of events (i.e. 1000 x total number of geological earthquakes recorded). In addition to providing information about earthquake parameters the PDFs for earthquake recurrence and slip were used to generate displacement vs time curves for each fault over time periods up to millions of years. These curves were created by randomly sampling a recurrence

interval and a slip increment from their respective PDFs and assigning the earthquake slip increment to the time at the end of the recurrence interval. This process was repeated 1000 times to produce stepped curves with vertical sections of a curve corresponding to an earthquake. The total duration of the model varied for each fault depending on average recurrence interval. On the Porters Pass Fault, for example, where the average recurrence interval is 1630 years the curve spans approximately 1.63 million years. In this report displacement-time curves for each fault have been used to examine temporal variations in COV. Displacement-time curves have also been used to assess the temporal variability of fault slip rates together with the utility of slip and time predictable models to forecast the timing of future earthquakes, but these results are beyond the scope of this report and are not presented.

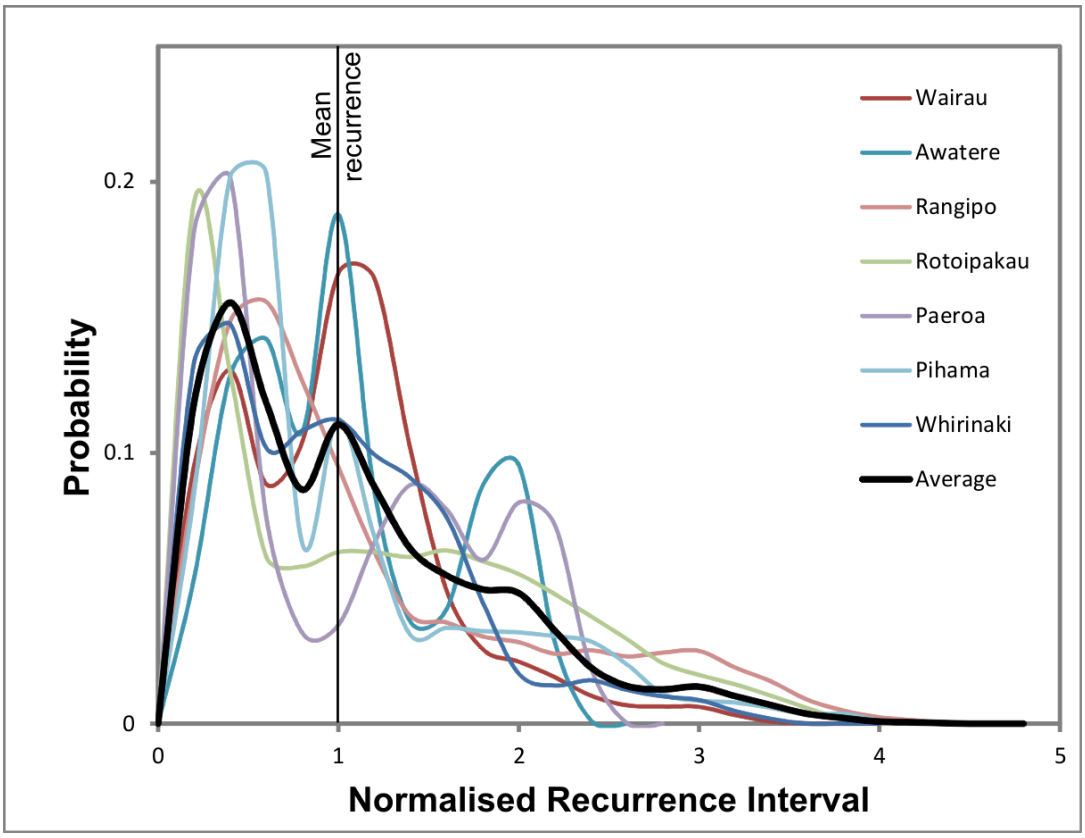

Figure 4.1 Probability Density Functions (PDF) for the 7 faults presented in Figure 2.4. To enable comparison of the PDFs for faults with different mean recurrence intervals the curves have been normalised to their mean (i.e. mean=1). The thick black line is the arithmetic mean of the 7 faults presented. Note that for the examples presented the most common recurrence interval is typically less than or equal to the average, while recurrence intervals a factor of 2-4 times the average are common.

The recurrence and slip histograms for natural earthquakes have been used in conjunction with, and compared to, histograms output for the same parameters from the synthetic seismicity models. Synthetic earthquake recurrence and slip populations have been presented for some of the faults in Table 2.1 that have been modelled. These synthetic earthquake populations are not directly comparable to the geological data because their Mc is significantly lower (e.g., ~M4-5 vs ~M6-7.5). The importance of the Mc for the recorded recurrence interval (whether it is estimated from geological or synthetic data) is illustrated in Figure 4.2 where values of average recurrence interval for synthetic earthquakes on the Wairau Fault increase with rising Mc. On this particular fault the mean recurrence intervals for synthetic and geological earthquakes would be comparable if the Mc was 7.1-7.2 (similar to the Mc 7.2±0.2 that could be inferred for the Wairau Fault from measurement of displaced geomorphology).

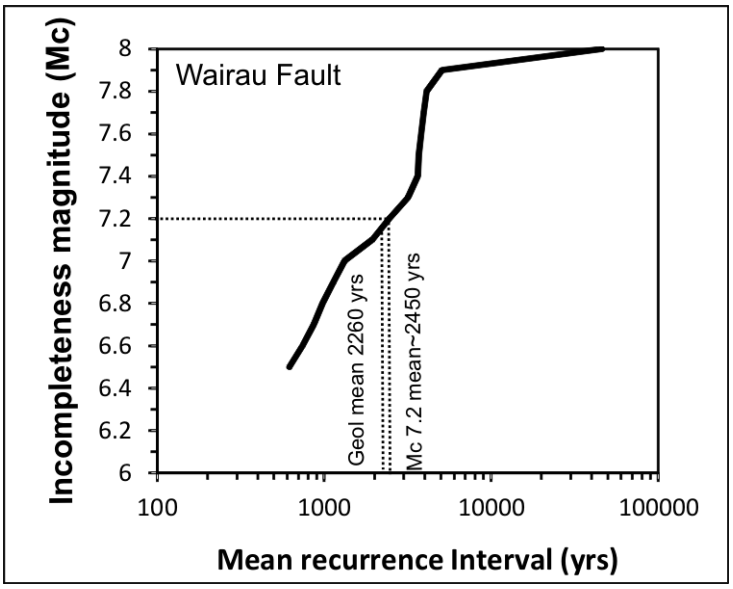

Figure 4.2 Positive relationship between the incompleteness magnitude (Mc) and the mean recurrence interval for synthetic earthquakes that ruptured anywhere on the Wairau Fault (i.e. includes events that do not rupture the ground surface or the entire fault). Note the similarity of mean synthetic recurrence for Mc 7.2 (~2450 yrs) and mean recurrence for geological paleoearthquakes (2260 yrs) which, using the data on the graph, would correspond with an Mc of about 7.15.

In addition to the frequency histograms and PDFs we have measured the Coefficient of Variation (COV) for recurrence interval and single event slip. The COV is a normalized measure of dispersion of a probability distribution that has been widely used in the paleoearthquake literature (e.g., McCalpin and Nishenko, 1996; Marco et al., 1996; Hecker and Abrahamson, 2002; Dawson et al., 2008; Mouslopoulou et al., 2009a; Robinson et al., 2009a; Little et al., 2010; Berryman et al., 2012). COV is a single number, which may or may not be ascribed uncertainties, that is well suited to being used for comparing the variability of recurrence intervals and single event slip between faults. COVs for recurrence intervals and single event slip range up to ~1.75 and indicate that single event slip and recurrence interval can vary from being periodic (COV=0), to random (COV=1) to clustered (COV>1). We have derived COVs from the geological data for all of the faults in Table 2.1 (recurrence and slip) and for all of the synthetic faults (recurrence only) generated for Wellington and Taupo Rift regional models (Robinson et al., 2009a, 2009b, 2011); 12 faults have both geological and synthetic model earthquake records. The geological COVs carry uncertainties of one standard error which were estimated by randomly locating sample windows of duration equal to the geological record on the stochastic displacement-time curves to derive a population of COVs for each fault. COVs for the synthetic models were derived from the Mc adjusted datasets. These COVs are plotted against the fault slip rate to examine whether there is a relationship between COV and fault size.

5.0 RESULTS

The results section is divided into two main sub-sections in which the variability of recurrence intervals and of single event slip are discussed. In each sub-section histograms/PDFs and COVs are examined for both geological and synthetic earthquakes.

5.1 RECURRENCE INTERVALS

Recurrence intervals record the time between successive earthquakes on individual faults. Paleoearthquake studies indicate that average recurrence intervals can vary dramatically between faults. For the faults in Table 2.1, for example, average recurrence intervals range from 130 to ~8540 years and are generally inversely related to fault slip rates. Globally recurrence intervals also vary on individual faults by up to a factor of ten or more (e.g., Sieh et al., 1989; Grant and Sieh, 1994; Marco et al., 1996; Dawson et al., 2003; Palumbo et al., 2004; Weldon et al., 2004; Mouslopoulou et al., 2009a). These variations on individual faults are the focus of this section.

5.1.1 Histograms and Probability Density Functions (PDF)

Frequency histograms of recurrence interval provide an indication of how this parameter varies for each fault studied (Figure 2.4 and Appendix 2). In Figure 4.1 we present PDFs for the New Zealand faults with paleoearthquake records including 7 or more events (these faults are also plotted on Figure 2.4), while Appendix 2 presents plots for the remaining faults in Table 2.1. One of the most striking features of the frequency histograms is that their shape is highly variable. This variability is particularly noticeable for the faults in Appendix 2 which contain the fewest number of paleoearthquakes (4-6 events). Some of the variability of recurrence intervals evident for the geological data may be due to the small sample size of events (for further discussion see next paragraph). Despite the variability in the PDFs some common first-order geometries apply to Figure 4.1. These PDFs comprise a mode that is less than or equal to the mean. In all but one case (Awatere Fault) in Figure 4.1 the distributions are asymmetrically disposed about the mean with a long recurrence interval low frequency tail that can exceed the mean by up to a factor of 4 (see also Figure 2.4).

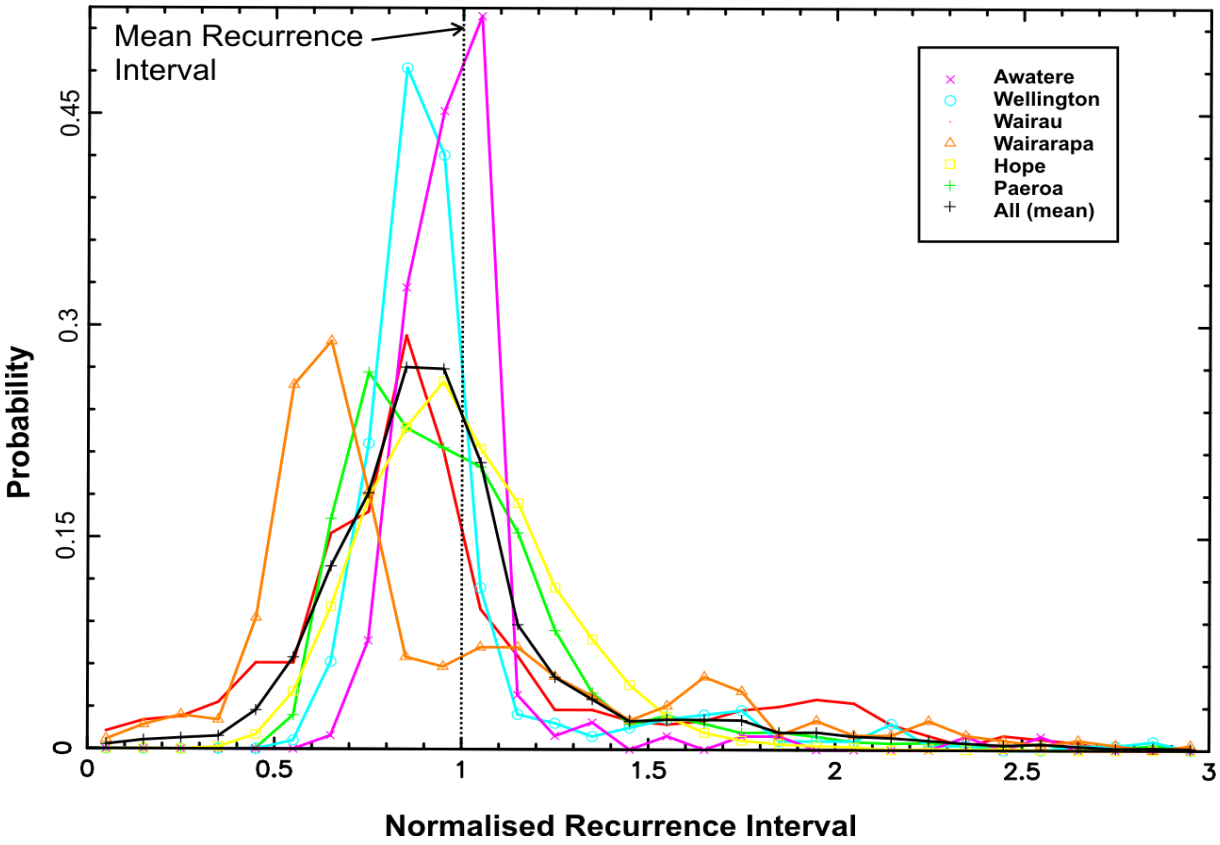

Figure 5.1 Recurrence interval PDFs for synthetic earthquakes on six faults (Awatere, Wellington, Wairau, Wairarapa, Hope, and Paeroa faults). For each fault events included in the plots are ≥Mc (for further discussion see section 2.2) and recurrence interval normalised to the mean (i.e. mean=1). Combined curve is the arithmetic mean of the curves for the individual faults.

The shapes of the geologically-derived frequency histograms and PDFs are more variable than those generated for the same faults using synthetic seismicity models. Figure 5.1, for example, shows PDFs from synthetic earthquakes for the six faults represented in Figure 4.1 that model outputs are available for. The curves in Figure 5.1 are (as with the natural earthquakes) slightly asymmetric with modes at, or slightly less than, the mean and a long recurrence interval tail which exceeds the mean by up to a factor of 3. There are also differences between the natural and synthetic curves, most noticeably that the latter are dominated by single modes and do not vary dramatically between faults. The greater stability of the synthetic earthquake curves could be attributed to the greater number of earthquakes underpinning the synthetic curves, the smaller uncertainties on recurrence in the models (compared to the geological data) and/or due to the models not precisely replicating the variability of natural faulting processes. The impact of the short duration of the geological sample interval is illustrated in Figure 5.2 where COV of recurrence for synthetic earthquakes on the Wairau fault varies from ~0.15 to >1 but is often less than the geological COV of 0.59. The amplitudes of curves like Figure 5.2 increase with decreases in the number of events in each bin (see also Parsons, 2008), supporting the view that the spread of recurrence interval variations could be expected to vary more for the geological than the synthetic samples.

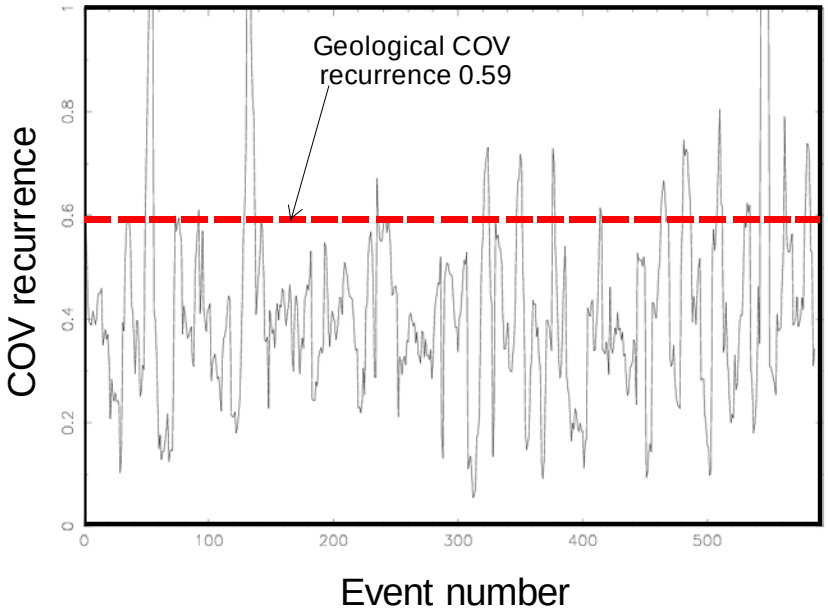

Figure 5.2 Variation in COV over time for sample windows of 7 synthetic earthquakes (≥ Mc ~7.5) on the Wairau Fault. This figure illustrates that the COV on a fault may change temporally.

5.1.2 Coefficient of Variation (COV)

The COV results are consistent with the frequency histograms of recurrence interval and support the view that this parameter varies for each fault studied. The variability of COV for recurrence intervals are shown in Figure 5.3 and Figure 5.4. COV of recurrence interval for the geological data ranges from ~0.2 to 1 and varies from being quasi periodic (~0.2-0.4) to quasi random (~0.7-1.0). The observed range of COVs estimated for this study are consistent with those calculated from paleoearthquakes on active faults internationally (e.g., McCalpin and Nishenko, 1996; Hecker and Abrahamson, 2002; Dawson et al., 2008; Mouslopoulou et al., 2009a). For example, COV of 0.5-0.75 has been calculated from recurrence intervals primarily measured for strike-slip faults, including the San Andreas Fault (e.g., Sieh et al., 1989; Ellsworth et al., 1999; Weldon et al., 2004). None of the geological recurrence intervals in this study are considered to be clustered using the COV criterion (i.e. COV>1), however, given the mean COV of 0.58 and a standard deviation of 0.2 a small proportion (~2-3%) of faults with clustered recurrence intervals might be expected if our geological sample were larger (Figure 5.3A). Such clustering would be consistent with the long recurrence tails (e.g., recurrence intervals > twice the mean) observed on many of the recurrence interval frequency histograms (e.g., Figure 4.1 and Appendix 2) which also generally account for a small proportion (e.g., <5%) of the total number of intervals. The small proportion of clustered recurrence intervals and a range of COV between ~0.2 and 1 is consistent with the suggestion that most (~95%) recurrence intervals are within a factor of two of the mean (i.e. COV ~0.2-1.0).

As is the case with the frequency histograms some of the variability of COV for recurrence interval for geological data could be due to the small sample numbers and/or the large errors on recurrence intervals. To test the significance of these sampling artefacts, in Figure 5.3B we present the COV for recurrence intervals for synthetic earthquakes from the Wellington and Taupo Rift regional models (Robinson et al., 2009a, 2009b and 2011). Comparison of Figure 5.3A and Figure 5.3B suggests that, to a first order, COV for natural and synthetic earthquakes is similar in range, mean and standard deviation. This broad equivalence, together with the fact that the COV of recurrence for New Zealand faults are similar to active faults from overseas, adds support to the view that our results are at least reproducible.

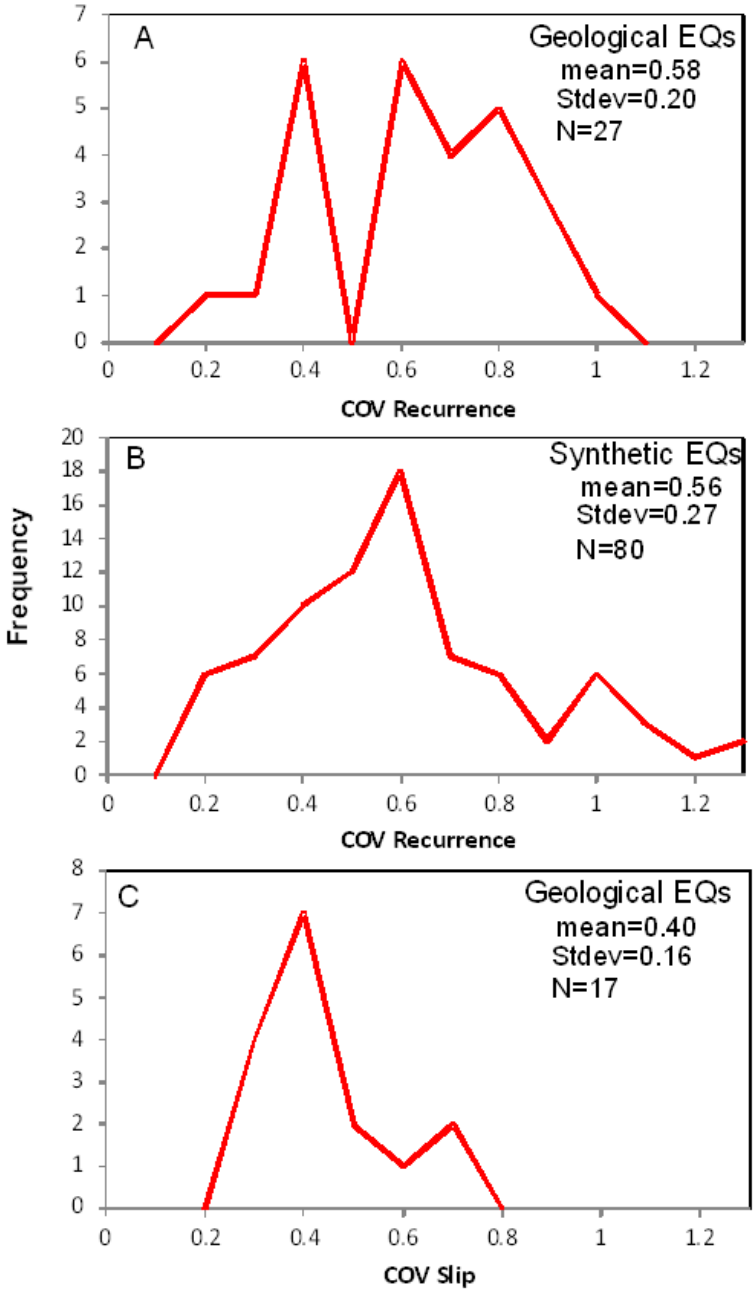

Figure 5.3 COV histograms for recurrence interval of geological earthquakes (A) and synthetic earthquakes (B) and for slip of geological earthquakes (C).

A significant question regarding COV for recurrence interval is does it vary systematically with fault size? Previous studies have suggested that COV may be inversely related to slip rate (e.g., Robinson et al., 2009a; Berryman et al., 2012), however, the datasets underpinning these inferences were limited in number. In Figure 5.4 we plot COV for recurrence interval against fault slip rate for geological earthquakes (white triangles) and synthetic earthquakes (red and green filled circles). Fault slip rates range in excess of two orders of magnitude (0.1 to 25 mm/yr, see Table 2.1 and Robinson et al. 2009a and 2009b for data) and COVs from ~0.1 to 1.25 for all synthetic and geological data. The natural and synthetic data produce comparable distributions on Figure 5.4, but may vary by up to ~0.5 for the same fault (e.g., Vernon Fault synthetic COV 0.1 and geological COV 0.6). Similar variability for different periods of time has been observed in the synthetic earthquake results (e.g., Figure 5.2) and could reflect sampling artefacts rather than suggesting that either geological or synthetic data are in error.

The data cloud in Figure 5.4 may be slightly elongate towards the top left-hand corner of the graph, suggesting the possibility of negative relationship between recurrence COV and slip rate (i.e. faster moving faults have lower COVs), however, the relationship is considered to be weak. The lower bound of the COV data does not appear to change with slip rate, while the same is also true of the upper bound of the data at slip rates of less than 2 mm/yr. At slip rates higher than 2 mm/yr the upper bound of the distribution appears to slope towards the right of the graph possibly suggesting a decrease in the range of COVs with increasing slip rate. A change in the slope of the upper bound of the distribution at slip rates >2 mm/yr would be consistent with suggestions that larger faults mainly respond to uniform plate motions and smaller faults to less uniform fault interactions (Robinson et al., 2009a; Berryman et al., 2012). However, testing this model is beyond the scope of the current report. For the purposes of this report we suggest that the relationship between recurrence COV and slip rate is too poorly defined to be incorporated into the NSHM (see Application to NSHM section for further discussion).

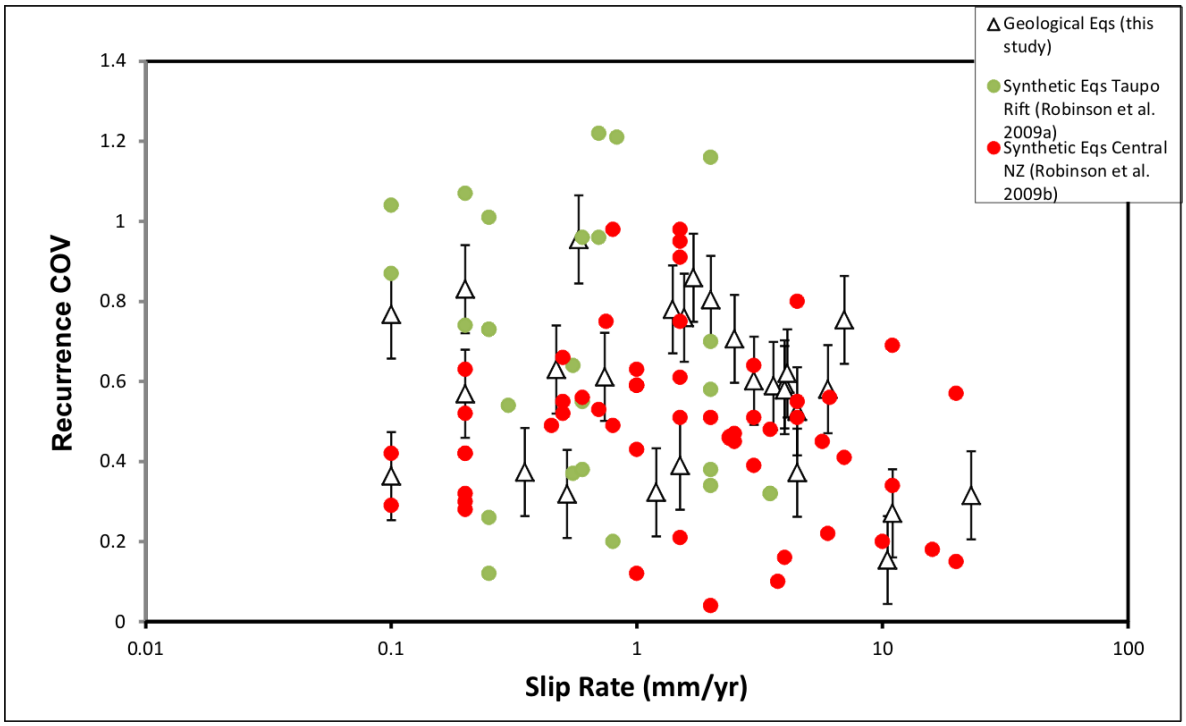

Figure 5.4 COV of recurrence interval vs slip rate for geological and synthetic large magnitude earthquakes.

5.2 SINGLE EVENT SLIP

Single event slip records the displacement that accrues during each surface-rupturing earthquake. Earthquake slip could range up to 18.5 m and has a positive relationship with magnitude (e.g., Wells and Coppersmith, 1994; Rodgers and Little, 2006). The faults presented in Table 2.1 range in average single event slip from 0.5 to 16.9 m, with the lower bound of these values probably being defined (or at least strongly influenced) by the detection limit of geological investigations. In New Zealand, single event slip on individual faults may be approximately uniform (Van Dissen and Nicol, 2009; Little et al., 2010; Townsend et al., 2010) or vary by up to a factor of 5 (Townsend et al., 2010; Nicol et al., 2010; Nicol et al., 2011b). Whether most faults adhere to the uniform or variable single event slip models, and under what geological conditions each of these models might apply, are yet to be resolved. The focus of this section is to provide some resolution to the variability of single event slip.

5.2.1 Histograms

Frequency histograms of single event slip provide an indication of how this parameter varies for ten of the faults in Table 2.1 (Figure 5.5). These faults provide single event slip for 5 or more surface-rupturing earthquakes and in terms of the number of events and the completeness of the slip record are considered to be the best of the available data. As is the case with the recurrence dataset the shape of the histograms varies between faults. Some of this variability of single event slip may be due to the small sample size of events and/or to the one-dimensional sampling. Multiple modes evident for the Cloudy and Paeroa faults may, for example, directly reflect the low sample number with each mode corresponding to a single event. The spread of the data in the histograms ranges between factors of 3 and 15, however, for the majority of the faults most of the slip events are within a factor of 2 of the mean (Figure 5.5).

Six of the histograms (Mangatete, Pihama, Porters Pass, Snowdon, Wairau and Whirinaki faults) have approximately normal distributions with a mean (red line) that coincides with the mode and a minimum value which is roughly equal to the lower limit of recordable slip. The remaining histograms (Cloudy, Paeroa, Rangipo and Vernon) may be better approximated by log-normal distributions, although other distributions are also possible given the geometries of the histograms. The shapes of the geologically-derived histograms are broadly consistent with those generated for the same faults using synthetic seismicity models. Figure 5.6, for example, shows PDFs for synthetic earthquakes from five faults, including the Wairau, Paeroa and Whirinaki faults shown in Figure 5.5. The frequency curves in Figure 5.6 are dominated by approximately normal distributions with modes approximately coincident with the mean. As was the case with the recurrence data the shapes of the synthetic histograms vary less than the histograms from the geological data. Again, this increase in stability has been attributed to the greater number and smaller uncertainties of earthquakes underpinning the synthetic curves.

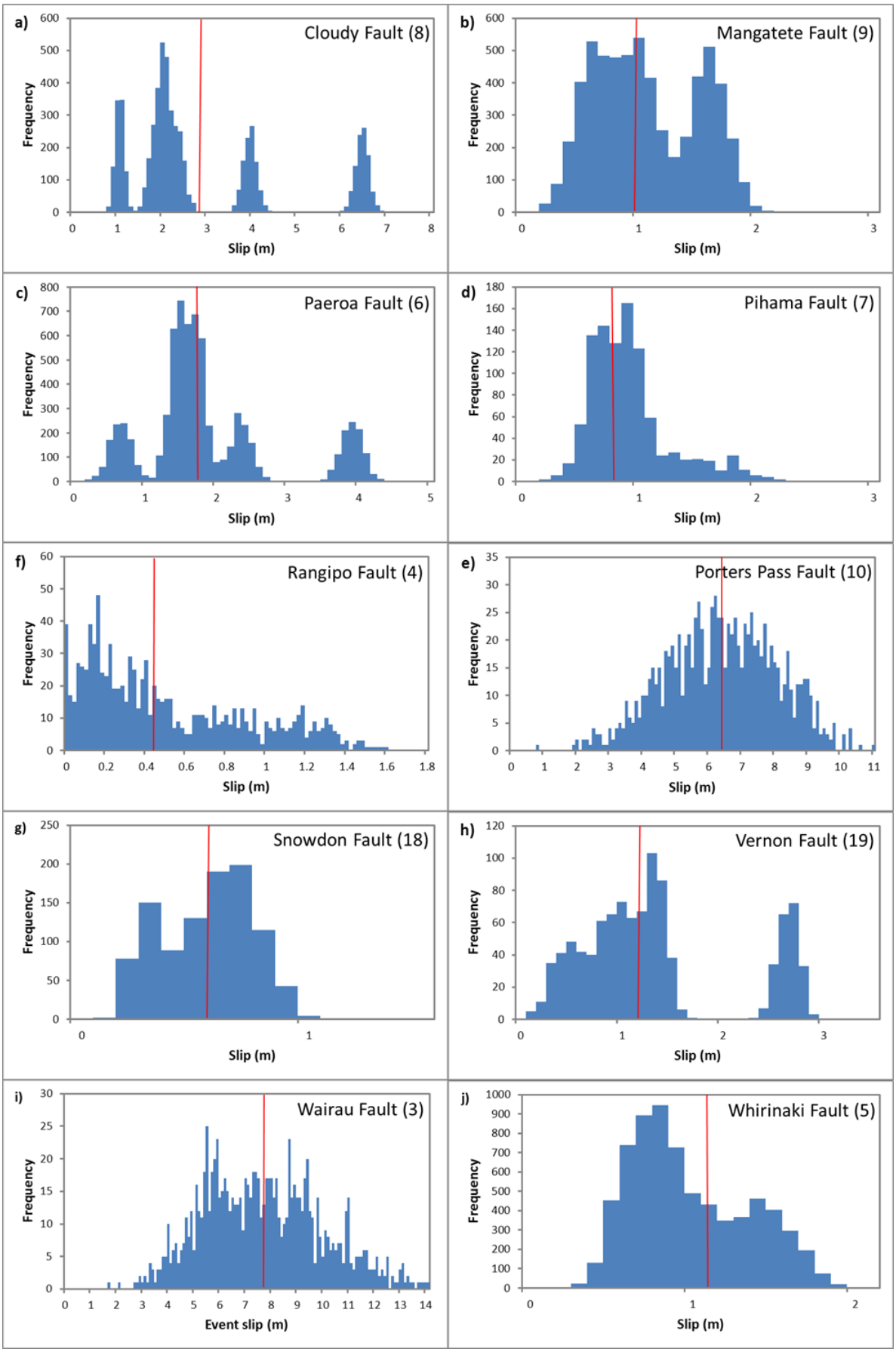

Figure 5.5 Histograms of single event slip for 10 active faults with 4 or more recorded earthquake slip values generated using the data in Appendix 1 and the Monte Carlo method outlined in the text. Red lines indicate the mean single event slip. For description of the faults see Table 2.1. Numbers beside fault name correlate with numbers assigned in Table 2.1 and Appendix 1.

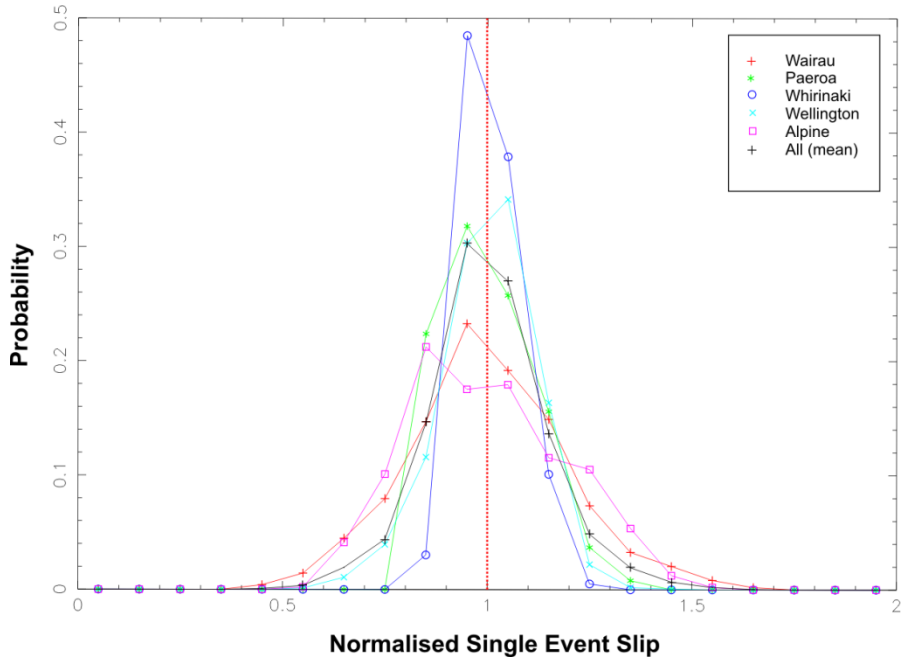

Figure 5.6 Histograms of single event slip from synthetic earthquake models for 5 of the active faults including the Wairau, Paeroa and Whirinaki faults shown in Figure 5.5. In each case the Single event slip has been normalised to the mean.

5.2.2 Coefficient of Variation (COV)

COV for single event slip derived from the geological data has a lesser spread than COV for recurrence interval (compare Figure 5.3A and Figure 5.3C). COV of single event slip for the geological data ranges from 0.25 to 0.75 with a mean of 0.4 and a standard deviation of 0.16. This mean (0.4) is significantly less than 0.58 calculated for recurrence intervals and suggests that single event slip is closer to being quasi periodic than quasi random. This conclusion is consistent with the COVs for individual faults which are typically lower for single event slip than for recurrence interval (e.g., Wairau Fault COV recurrence interval 0.59 and single event slip 0.31 for geological data; Appendix 1). The question remains, however, to what extent the lower bound of the slip distribution for surface-rupturing faults is influenced by the Mc (i.e. it is possible that some single event slip events will be too small to be routinely observed in the geological record). On strike slip faults, for example, surface-rupturing paleoearthquakes in New Zealand with <3 m single event slip will often be difficult to identify using displacement of landforms (e.g., terrace risers and abandoned stream channels). Being unable to sample these smaller displacements would remove them from the frequency histogram, biasing the data towards larger events and decreasing the slip COV. The potential impact of sampling on the frequency of smaller events is illustrated in Figure 5.7 by the histograms of average single event slip for synthetic events that ruptured the ground surface (A), Mc 7.2 events (i.e. ≥M 7.2) anywhere on the fault surface (B) and Mc 6.5 (≥M 6.5) anywhere on the fault surface (C). Figure 5.7A and Figure 5.7B are similar to each other (with modes of 5.5 m) and to the single event slip histogram for geological data on the Wairau Fault in Figure 5.5. The similarity of synthetic and geological data supports the view that the model results are approximately replicating nature. In addition, the similarity of Figure 5.7A and Figure 5.7B is consistent with the notion that ≥M 7.2 synthetic earthquakes on the Wairau Fault dominate surface-rupturing events and typical rupture its central segment. By contrast Figure 5.7A and Figure 5.7B differ significantly from Figure 5.7C which has a mode of 2.5 m. This leftward shift in the mode and the frequency histogram between Figure 5.7A, Figure 5.7B and Figure 5.7C is interpreted to be largely due to a decrease in Mc from 7.2 to 6.5. Figure 5.7C confirms the presence of many small slip (<3m) events in the

synthetic earthquake population, events which do not rupture the ground surface and are unlikely to be recorded in the geological record. If the data in Figure 5.7 are representative of geological record for the Wairau Fault, then smaller (i.e. sub-resolution) slip events could be up to a factor of six more frequent than the slip events recorded in the geological sample and points to the potential for a significant sampling bias which would reduce the variability and COV of single event slip. Such a sampling bias may mean that geological samples could appear quasi-Characteristic in part because the geological dataset is biased towards a relatively narrow size range of the earthquake magnitude population.

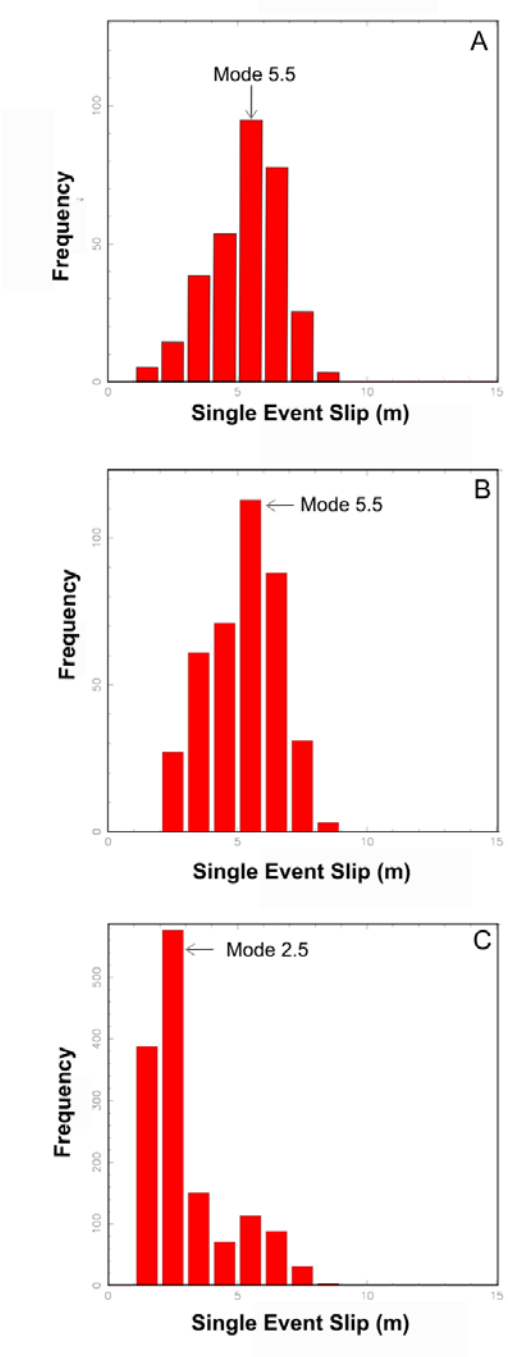

Figure 5.7 Single event slip histograms for synthetic earthquakes on the Wairau Fault. (A) Average slip for all earthquakes that ruptured the ground surface in the central section of the fault trace, (B) average slip for earthquakes of Mc 7.2 that ruptured anywhere on the fault surface (i.e. they need not rupture the ground surface or the central section of the fault) and, (C) average slip for earthquakes of Mc 6.5 that ruptured anywhere on the fault surface (i.e. they need not rupture the ground surface or the central section of the fault). Inclusion of smaller events shows a significant decrease in the modes between the upper two graphs and the lower histogram.

6.0 APPLICATION TO SEISMIC HAZARD ASSESSMENT

One of the primary reasons for collecting and analysing paleoearthquake data is for seismic hazard assessment. The New Zealand National Seismic Hazard model (NSHM) has been used as the hazard basis for the New Zealand Loadings Standard and for a range of other applications including assessment of infrastructural vulnerability to seismic events. Presently recurrence interval and single event slip of large magnitude prehistoric earthquakes on active faults are not input parameters for the NSHM (Stirling et al., 2002, 2007, 2012; Bradley et al., 2012). In the current version of the NSHM slip rates are input into the model and recurrence intervals and single event displacements are derived from fault length using standard empirical scaling relationships. An important objective of this research is to ensure that a description of variability of recurrence interval and single event slip for large magnitude earthquakes can be included in the New Zealand NSHM. Currently the NSHM does not take account of uncertainties (epistemic or aleatory), but rather uses estimated mean values for single event slip and recurrence interval on each active fault (Stirling et al., 2002, 2007, 2012). For many of the >530 active faults in the NSHM insufficient direct measurements of paleoearthquakes are available to constrain recurrence interval and/or single event slip and in such cases these values are estimated using fault length, empirical scaling relationships and/or fault slip rates. Here we consider whether, based on the current dataset, PDFs and COVs for single event slip and recurrence interval could be used to improve estimates of their variability and whether it is appropriate to input this variability into the NSHM.

PDFs have been estimated for recurrence intervals using both geological earthquakes and synthetic earthquakes. For the geological data the average PDF from Figure 4.1 has been plotted with best-fit log-normal and Weibull distributions in Figure 6.1A. Visual inspection of the curves suggests that the Weibull distribution may fit the data best, however, the difference between log-normal and Weibull distributions is small compared to the variations between PDFs for individual faults. In addition, the average PDF for synthetic recurrence intervals (Figure 6.1B) differs from that of the geological data and is also relatively poorly fit by log-normal and Weibull distributions. Differences between the geological and synthetic earthquake recurrence interval distributions together with their poor fit to the selected distributions suggest that more data and further analysis is required before the most appropriate recurrence interval PDFs can be identified and incorporated into the NSHM.

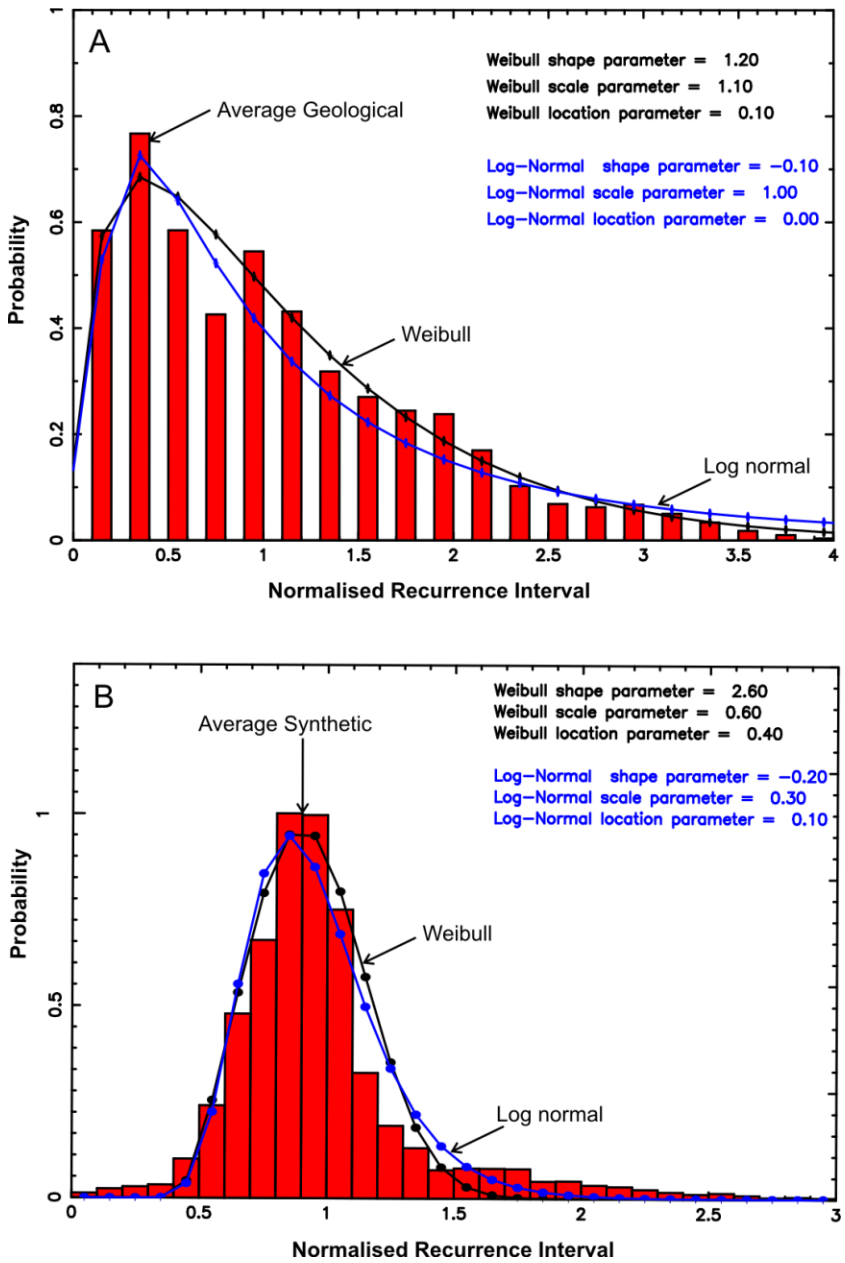

Figure 6.1 (A) Average recurrence PDF for geological data (red bars) plotted with best-fit log-normal and Weibull distributions. (B) Average PDF for synthetic recurrence intervals from six faults (Figure 5.1) plotted with normal, log normal and Weibull best-fit distributions.

In contrast to the recurrence interval PDFs the recurrence COVs for both geological data and synthetic earthquakes produce comparable results which are also similar to international COV compilations from paleoearthquake data (e.g., Sieh et al., 1989; McCalpin and Nishenko, 1996; Hecker and Abrahamson, 2002; Weldon et al., 2004; Dawson et al., 2008). Based on the models and data presented in this report we suggest that a mean recurrence COV of 0.60 with a standard deviation of 0.25 would be appropriate for the purposes of constructing probablistic seismic hazard models. This COV could be applied to all active faults for which insufficient data (e.g., 4 or more paleoearthquakes) are available to calculate a COV. The use of an active fault specific COV may be most important for the highest slip rate faults (e.g., Alpine Fault) which could be quasi periodic with COVs less 0.5. Whatever the precise value of COV adopted it should be acknowledged that it can only provide a first-order indication of the variability. This is partly because the PDFs appear to be better described by a log-normal distribution (as opposed to a normal distributed) which is not precisely described by a mean and a standard deviation.

Single event slip data for paleoearthquakes are less numerous than recurrence interval information. Given this paucity of data a PDF has not been developed for single event slip. It is noted however that for many of the active faults the geological and synthetic PDFs are approximately normally distributed and would be reasonably well described by COV. Based on the geological data single event slip for those earthquakes that rupture the ground surface (and are recorded in the geological record) may be quasi-Characteristic with a mean COV of 0.4 and a standard deviation of 0.2. Whether this COV accurately describes the spread of single event slip for all large magnitude events (i.e. including those that rupture the fault but are not preserved in the geological record) remains a question for further enquiry.

Uncertainties in earthquake parameters arising from sampling artefacts can be addressed by quoting COVs with a minimum magnitude of completeness (Mc). COV for single event slip (0.4±0.2) and recurrence interval (0.6±0.25) are inferred to have Mc of 7.2±0.2 and 6.1±0.2 for strike slip faults and normal faults, respectively. Too few data are presently available to assign Mc values for reverse faults, however, as earthquakes on these structures are often associated with folding of the ground surface rather than fault slip, they may also be characterised by larger Mc values (e.g., >M 7). Estimates of Mc can be significantly improved on what is presented here and should form a component of paleoearthquake investigations. Characterisation of Mc values will permit earthquakes not sampled by the geological record to be identified and input into NSHM seismicity models using alternative methods.

7.0 CONCLUSIONS

Recurrence intervals and single event slip for large magnitude earthquakes that ruptured the ground surface can vary by more than an order of magnitude on individual faults. To quantify this variability we use a combination of existing geological observations and synthetic earthquakes generated by numerical models for over 100 active faults in New Zealand. Synthetic earthquakes help fill information gaps in the natural data which may arise due to measurement uncertainty and to the brevity of the geological record (i.e. <10 surface-rupturing earthquakes per fault). These datasets define frequency histograms and probability density functions (PDFs) for recurrence interval and single event slip. They are also used to define the coefficient of variation (COV) for recurrence interval and single event slip. Although the shapes of histograms generated for recurrence intervals from geological data using a Monte Carlo method are variable, for the best data (i.e. ≥7 events) they are often asymmetric with modes less than, or equal to, the mean and a long recurrence (3-4 times the mean) tail. The resulting PDFs for recurrence more closely resemble log-normal or Weibull than normal distributions, in contrast to the single event slip for geological data which in many cases is approximately normal. Recurrence interval histograms for synthetic earthquakes show less variability between faults than the geological data, which may be partly due to the significantly larger number of events in the synthetic dataset. Histograms and PDFs for synthetic earthquakes are similar to the geological data in that they exhibit a long recurrence interval tail. COV for recurrence interval (0.58±0.20 geological and 0.56±0.27 synthetic) and single event slip (0.40±0.20 geological) suggest that recurrence could be more variable that single event slip. COV for single event slip (0.4±0.2) and recurrence interval (0.6±0.25) are recommended for the NSHM given magnitudes of completeness (Mc) of about 7.2±0.2 and 6.1±0.2 for strike slip faults and normal faults, respectively. More data and analysis are required however to quantify the minimum magnitude of completeness for geological data and to understand better how this may be impacting on the results. Despite these outstanding questions COV for recurrence interval and single event slip provide constraints on the variability of these parameters and could be applied to active faults for which there are insufficient data to constrain the paleoearthquake history. The results of this work are preliminary and more research is required to define better the PDFs for recurrence interval and single event slip before these can be input into the National Seismic Hazard Model.

8.0 ACKNOWLEDGEMENTS

This report utilises the research of many paleoseismologists mostly conducted over the last 20 years and without which this work would not have been possible. Rob Langridge and Annemarie Christophersen are thanked for their thorough reviews of the report. The research reported in this document was mainly funded by a biennial EQC research grant (EQC Project BI10/596).

9.0 REFERENCES

Barnes, P.M., Pondard, N. 2010. Derivation of direct on-fault submarine paleoearthquake records from high-resolution seismic reflection profiles: Wairau Fault, New Zealand. *Geochemistry, Geophysics, Geosystems* 11, Q11013, doi:10.1029/2010GC003254.

Barnes, P.M., Nicol, A., Harrison, T., 2002. Late Cenozoic evolution and earthquake potential of an active listric thrust complex, Hikurangi subduction margin, New Zealand. Geol. Soc. Am. Bull.114, 1379-1405.

Begg, J.G., Mouslopoulou, V., 2010. Analysis of late Holocene faulting within an active rift using lidar, Taupo Rift, New Zealand, Journal of Volcanology and Geothermal Research 190, 152-167; doi:10.1016/j.jvolgeores.2009.06.001

Ben-Zion, Y., 1996. Stress, slip and earthquakes in models of complex single-fault systems incorporating brittle and creep deformation. Journal of Geophysical Research 101, 5677-5708.

Ben-Zion, Y., Dahmen, K., Lyakhovsky, V., Ertas, D., Agnon, A., 1999. Self-driven mode switching of earthquake activity on a fault system. Earth and Planetary Science Letters 172, 11-21.

Benson, A.M., Little, T.A., Van Dissen R.J., Hill N., Townsend D.B., 2001. Late Quaternary paleoseismicity and surface rupture characteristics of the eastern Awatere strike-slip fault, New Zealand. Geological Society of America Bulletin 113(8), 1079-1091.

Berryman, K.R., 1993. Age, Height and Deformation of Holocene marine terraces at Mahia Peninsular, Hikurangi subduction margin, New Zealand. Tectonics 12 (6), 1347-1364

Berryman, K.R., Beanland, S., Wesnousky, S., 1998. Paleoseismicity of the Rotoitipakau Fault Zone, a complex normal fault in the Taupo Volcanic Zone, New Zealand. New Zealand Journal of Geology and Geophysics 41, 449-465.

Berryman, K., Villamor, P., Nairn, I., Van Dissen, R., Begg, J., Lee, J., 2008. Late Pleistocene surface rupture history of the Paeroa Fault, Taupo Rift, New Zealand. New Zealand Journal of Geology and Geophysics 51, 135–158.

Berryman, K., Cochran, U.A., Clark, K.J., Biasi, G.P., Langridge, R.M., Villamor, P., 2012. Major Earthquakes Occur Regularly on an Isolated Plate Boundary Fault. *Science* 336, 1690 (2012); doi: 10.1126/science.1218959.

Biasi, G.P., Weldon, R.J., 2006. Estimating Surface Rupture Length and Magnitude of Paleoearthquakes from Point Measurements of Rupture Displacement. Bulletin of the Seismological Society of America 96, 5, pp. 1612–1623, doi: 10.1785/0120040172.

Bradley, B.A., Stirling, M.W., McVerry, G.H., Gerstenberger, M., 2012. Consideration and Propagation of Epistemic Uncertainties in New Zealand Probablitistic Seismic-Hazard Analysis. Bulletin of the Seismological Society of America 102, 4, pp. 1554–1568, doi: 10.1785/0120140257.

Canora-Catalán, C., Villamor, P., Berryman, K., Martínez-Diaz, J.J., Raen, T., 2008. Rupture history of the Whirinaki Fault, an active normal fault in the Taupo Rift, New Zealand. New Zealand Journal of Geology and Geophysics 51, 277-293.

Cowan H.A., McGlone, M.S., 1991. Late Holocene displacements and characteristic earthquakes on the Hope River segment of the Hope Fault, New Zealand. Journal of the Royal Society of New Zealand 21, 4, 373-384.

Dawson, T.E., McGill, S.F., Rockwell, T.K., 2003. Irregular recurrence of paleoearthquakes along the central Garlock Fault near El Paso Peaks, California. Journal of Geophysical Research, 108 (B7), 2356. doi:10.1029/2001JB001744.

Dawson, T.E., Weldon, R.J., II, Biasi, G.P., 2008. Recurrence interval and event age data for Type A faults, Appendix B in The Uniform California Earthquake Rupture Forecast, version 2 (UCERF 2): U.S. Geological Survey Open-File Report 2007-1437B and California Geological Survey Special Report 203B, 48 p. [http://pubs.usgs.gov/of/2007/1437/b/].

Downs, G.L., in press. Update of Atlas of Isoseismal maps of new Zealand earthquakes. GNS Sceince monograph, Lower Hutt, New Zealand.

Friedrich, A.M., Wernicke, B.P., Niemi, N.A., Bennett, R.A., Davis, J.L., 2003. Comparison of geodetic and geologic data from the Wasatch region, Utah, and implications for the spectral character of Earth deformation at periods of 10 to 10 million years. Journal of Geophysical Research 108, B4, 2199, doi:10.1029/2001JB000682, 2003.

Fitzenz, D., Miller, S., 2001. A forward model for earthquake generation on interacting faults including tectonics, fluids, and stress transfer. Journal of Geophysical Research 106, 26,689-26,706.

Grant, L. B., Sieh, K., 1994. Paleoseismic evidence of clustered earthquakes on the San Andreas fault in the Carrizo Plain, California. Journal of Geophysical Research 99, 6819–6841.

Grapes, R.H., Wellman, H.W. 1986. The north-east end of the Wairau Fault, Marlborough, New Zealand. Journal of the Royal Society of New Zealand 16, 245-250.

Harris, R., 1998. Introduction to special section: Stress triggers, stress shadows, and implications for seismic hazard. Journal of Geophysical Research 103, 24, 347-24,358.

Hecker, S., Abrahamson, N., 2002. Characteristic fault rupture: implications for rupture hazard analysis, paper presented at Pacific Earthquake Engineering Research Centre (PEER) Lifelines Research meeting, Oakland, California, June 24, 2002.

Hemphill-Haley, M. A., Weldon R.J., 1999. Estimating prehistoric earthquake magnitude from point measurements of surface rupture, Bulletin of the Seismological Society of America 89(5), 1264–1279.

Heron, D., Van Dissen, R., Sawa, M., 1998. Late Quaternary movement on the Ohariu Fault, Tongue Point to MacKays Crossing, North Island, New Zealand. New Zealand Journal of Geology & Geophysics 41, 419–439.

Howard, M., Nicol, A., Campbell, J.K., Pettinga. J.R., 2005. Prehistoric earthquakes on the strike-slip Porters Pass Fault, Canterbury, New Zealand. New Zealand Journal of Geology & Geophysics 48, 59-74.

King, G., Cocco, M., 2000. Fault Interaction by Elastic Stress Changes: New Clues from Earthquake Sequences. Advances in Geophysics 44, 1-36.

Langridge, R.M., Van Dissen, R., Rhoades, D., Villamor, P., Little, T., Litchfield, N.,R., Clark, K., Clark, D., 2011. Five thousand years of surface ruptures on the Wellington Fault, New Zealand: Implications for recurrence and fault segmentation. Bulletin of the Seismological Society of America 101 (5), doi:10.1785/0120100340.

Lettis, W.R., Wells, D.L., Baldwin, J.N., 1997. Empirical observations regarding reverse earthquakes, Blind thrust faults and Quaternary deformation: are blind thrust faults truly blind? Bulletin of the Seismological Society of America 87 (5), 1171-1198.

Litchfield, N.,Van Dissen, R., Heron, D., Rhoades, D., 2006. Constraints on the timing of the three most recent surface rupture events and recurrence interval for the Ohariu Fault: trenching results from MacKays Crossing, Wellington, New Zealand. New Zealand Journal of Geology & Geophysics 49, 57–61.

Litchfield, N., Van Dissen, R., Hemphill-Haley, M., Townsend, D. Heron, D., 2010. Post c. 300 year rupture of the Ohariu Fault in Ohariu Valley, New Zealand. New Zealand Journal of Geology & Geophysics 53, 43–56.

Little, T.A., Van Dissen, R., Schermer, E. Carne, R., 2009. Late Holocene surface ruptures on the southern Wairarapa fault, New Zealand: Link between earthquakes and the uplifting of beach ridges on a rock coast. Lithosphere 1, 4-28, doi: 10.1130/L7.1.

Little, T.A., Van Dissen, R., Rieser, U., Smith, E.G.C., Langridge, R.M., 2010. Coseismic strike slip at a point during the last four earthquakes on the Wellington fault near Wellington, New Zealand. Journal of geophysical Research, 115, B05403, doi:10.1029/2009JB006589, 2010.

McCalpin, J., 1996. Paleoseismology. Academic Press, New York, 588 pp.

McCalpin, J.P., Nishenko, S.P., 1996. Holocene paleoseismicity, temporal clustering, and probabilities of future large (M>7) earthquakes on the Wasatch fault zone, Utah. Journal of Geophysical Research 101, 6233-6253.

Marco, S., Stein, M., Agnon, A., 1996. Long-term earthquake clustering: A 50,000-year paleoseismic record in the Dead Sea Graben. Journal of Geophysical Research 101, B3, 6179-6191.

Mason, D., Little, T.A., Van Dissen, R.J., 2006. Refinements to the paleoseismic chronology of the eastern Awatere Fault from trenches near Upcot Saddle, Marlborough, New Zealand. New Zealand Journal of Geology and Geophysics 49, 383-397.

Mouslopoulou, V., 2006. Quaternary geometry, kinematics and paleoearthquake history at the intersection of the strike-slip North Island Fault System and Taupo Rift, New Zealand. PhD Thesis. Victoria University of Wellington, New Zealand.

Mouslopoulou, V., Walsh, J.J., Nicol, A., 2009a. Fault displacement rates on a range of timescales. Earth and Planetary Science Letters 278, 186-197.

Mouslopoulpou, V., Nicol, A., Little, T. A., Begg, J. G., 2009b. Paleoearthquake surface rupture in a transition zone from strike-slip to oblique-normal slip and its implication to seismic hazard, North Island Fault System, New Zealand. In: Historical and Pre-historical Records of Earthquake Ground Effects for Seismic Hazard Assessment. Geological Society, London, Special Publication 316, 269-292 doi:10.1144/SP316.17.

Mouslopoulou, V., Nicol, A., Walsh, J.J., Begg, J., Townsend, D., Hristopulos, D.T., 2012. Fault-slip accumulation in an active rift over thousands to millions of years and the importance of paleoearthquake sampling. Journal of Structural Geology, Online first: doi: 10.1016/j.jsg.2011.11.010.

Nicol, A., Villamor, P., Berryman, K., Walsh, J., 2007. Variable paleoearthquake recurrence intervals arising from fault interactions, Taupo Rift, New Zealand. IUGG XXIV2007 Perugia Italy, July 2-13, 2007.

Nicol, A., Walsh, J.J., Mouslopoulou, V., Villamor, P., 2009. Earthquake histories and an explanation for Holocene acceleration of fault displacement rates. Geology 37 (10), 911–914; doi: 10.1130/G25765A.

Nicol, A., Begg, J., Mouslopoulou, V., Stirling, M., Townsend, D., Van Dissen, R., Walsh, J., 2011a. Active faults in New Zealand: what are we missing? In: Litchfield, N.J., Clark, K. (eds). Abstract Volume, Geosciences 2011 Conference, Nelson, New Zealand. Geoscience Society of New Zealand Miscellaneous Publication 130A: p. 79. ISBN 978-1-877480-13-3.

Nicol, A., Langridge, R., Van Dissen, R., 2011b. Wairau Fault: Late Quaternary displacements and paleoearthquakes. p. 5-67 In: Lee, J.M. (ed.): Field trip guides, Geosciences 2011 Conference, Nelson, New Zealand. Geoscience Society of New Zealand miscellaneous publication 130B, 33 p. ISBN 978-1-877480-14-0.

Ota, Y., Beanland, S., Berryman, K.R., Nairn, I.A., 1988. The Matata Fault: active faulting at the north-western margin of the Whakatane Graben, Eastern Bay of Plenty. Research Notes, New Zealand Geological Survey Record 35, 6–13.

Okada, Y., 1992. Internal deformation due to shear and tensile faults in a half-space. Bulletin of the Seismological Society of America 82, 1018-1040.

Palumbo, L., Benedetti, L., Bourles, D., Cinque, A., Finkel, R., 2004. Slip history of the Magnola fault (Appennines, Central Italy) from 36Cl surface exposure dating: evidence for strong earthquakes over the Holocene. Earth and Planetary Science Letters, 225, 163-176.

Parsons, T., 2008. Monte Carlo method for determining earthquake recurrence parameters from short paleoseismic catalogs: Example calculations from California. Journal of Geophysical Research 113 (B03302), doi:10.1029/2007JB004998,2008.

Pondard, N., Barnes, P.M. 2010. Structure and paleoearthquake records of active submarine faults, Cook Strait, New Zealand: Implications for fault interactions, stress loading, and seismic hazard. Journal of Geophysical Research 115 (B12320), doi:10.1029/2010JB007781.

Pondard, N., Armiji, R., King, G., Meyer, B., Flerit, F., 2007. Fault Interactions in the Sea of Maramara Pull-Apart (North Anatolian Fault): Earthquake Clustering and Propagating Earthquake Sequences. Geophysical Journal International 171, 1185-1197.

Quigely, M., Van Dissen, R., Litchfield, N., Villamor, P., Duffy, B., Barrell, D., Furlong, K., Stahl, T., Bilderback, E., Noble, D., 2012. Surface rupture during the 2010 Mw 7.1 Darfield (Canterbury) earthquake: implications for fault rupture dynamics and seismic-hazard analysis. Geology 40, 1, 55-58: doi:10.1130/G32528.

Robinson, R., 2004. Potential Earthquake Triggering in A Complex Fault Network: The Northern South Island, New Zealand. Geophysical Journal International 159, 734-748.

Robinson, R., Benites, R., 1996. Synthetic Seismicity Models for the Wellington Region, New Zealand: Implications for the Temporal Distribution of Large Events, Journal of Geophysical Research 101, 27,833-27,845.

Robinson, R., Benites, R., 2001. Upgrading a synthetic seismicity model for more realistic fault ruptures. Geophysical Research Letters, 28, 1843-1846.

Robinson, R., Nicol, A., Walsh, J.J., Villamor, P., 2009a. Features of Earthquake Occurrence in a complex normal fault network: results from a synthetic seismicity model of the Taupo Rift, New Zealand. Journal of Geophysical Research 114, B12306, doi:10.1029/2008JB006231.

Robinson, R., Van Dissen, R., Litchfield, N., 2009b. It's Our Fault – Synthetic Seismcity of the Wellington Region: Final Report. GNS Science Consultancy Report 2009/192, July 2009.

Robinson, R., Van Dissen, R., Litchfield, N., 2011. Using synthetic seismicity to evaluate seismic hazard in the Wellington region, New Zealand. Geophysical Journal International 187, 510-528; doi:10.1111/j.1365-246X.2011.05161.x

Rodgers, D.W., Little, T.A., 2006. World's largest coseismic strike-slip offset: The 1855 rupture of the Wairarapa Fault, New Zealand, and implications for displacement/length scaling of continental earthquakes, Journal of Geophysical Research 111, B12408, doi:10.1029/2005JB004065.

Rundle, P., Rundle, J., Tiampo., K., Donnellan, A., Turcotte, D., 2006. Virtural California: fault model, frictional parameters, applications, Pure and Applied Geophysics 163, 1819-1846.

Schwartz, D. P., Coppersmith, K.J.,1984. Fault behavior and characteristic earthquakes: Examples from the Wasatch and San Andreas Fault zones, Journal of Geophysical Research 89, 5681–5698, doi:10.1029/JB089iB07p05681.

Sieh, K.E., Stuiver, M., Brillinger, D., 1989. A more precise chronology of earthquakes produced by the San Andreas fault in southern California. Journal of Geophysical Research 94, 603-623.

Somerville, P., Irikura, K., Graves, R., Sawada, S., Wald, D., Abrahamson, N., Iwasaki, Y., Kagawa, T., Smith, N., Kowada, A., 1999. Characterizing crustal earthquake slip models for the prediction of strong ground motion. Seismological Research Letters 70, 59-80.

Stirling, M.W., McVerry, G.H., Berryman, K.R.., 2002. A new seismic hazard model for New Zealand. Bulletin of the Seismological Society of America 92, 1878-1903.

Stirling, M.W., Earthquake Hazards Team, 2007. Updating the national seismic hazard model for New Zealand. Paper 072 In: Conference proceedings, 8th Pacific Conference on Earthquake Engineering, 5-7 Dec 2007, Singapore. Singapore: 8PCEE.

Stirling, M., McVerry, G., Gerstenberger, M., Litchfield, N., Van Dissen, R., Berryman, K., Barnes, P., Wallace, L., Villamor, P., Langridge, R., Lamarche, G., Nodder, S., Reyners, M., Bradley, B., Rhodes, D., Smith, W., Nicol, A., Pettinga, J., Clark, K., Jacobs, K., 2012. National Seismic Hazard Model for New Zealand: 2010 Update. Bulletin of the Seismological Society of America 102, 4, 1514–1542, doi: 10.1785/0120110170.

Townsend, D., Nicol, A., Mouslopoulou, V., Begg, J.G., Beetham, R.J., Clark, D., Giba, M., Heron D., Lukovic, B., Macphearson, A., Seebeck, H., Walsh, J.J. 2010 paleoearthquake histories of a normal fault system in the southwestern taranakin Peninsula, New Zealand. NewZealand Journal of Geology and Geophysics 53, 4, 375-394.

Van Dissen, R.J., Nicol, A., 2009. Mid-late Holocene paleoseismicity of the middle Clarence valley section of the Clarence Fault, Marlborough, New Zealand. New Zealand Journal of Geology & Geophysics 52, 195-208.

Villamor, P., Van Dissen, R.J., Alloway, B.V., Palmer, A.S., Litchfield, N.J., 2007. The Rangipo Fault, Taupo rift, New Zealand: an example of temporal slip-rate and single-event displacement variability in a volcanic environment. Bulletin of the Geological Society of America 119, 529-547

Wallace, R.E., 1987. Grouping and migration of surface faulting and variations in slip rates on faults in the Great Basin Province. Bulletin of the Seismological Society of America 77, 868-876.

Ward, S. 2000. San Francisco Bay Area earthquake simulations: a step toward a standard physical earthquake model. Bulletin of the Seismological Society of America 90, 370 - 386.

Weldon, R., Scharer, K., Fumal, T., Biasi, G., 2004, Wrightwood and the earthquake cycle: what a long recurrence record tells us about how faults work. GSA Today 14, doi: 10.1130/1052-5173(2004)014<4:WATECW>2.0.CO:2.

Wells, A., Yetton, M.D., Duncan, R.P., Stewart, G.H., 1999. Prehistoric dates of the most recent Alpine fault earthquakes, New Zealand. Geology 27, 995-998.

Wells, A., Goff, J., 2007. Coastal dunes in Westland, New Zealand, provide a record of paleoseismic activity on the Alpine fault. Geology 35, 731-734; doi: 10.1130/G23554A.1.

Wells, D. L., Coppersmith, K.J., 1993. Likelihood of surface rupture as a function of magnitude. Seismological Research Letters 64, 54.

Wells, D. L., Coppersmith, K.J., 1994. New empirical relationships among magnitude, rupture length, rupture width, rupture area, and surface displacement. Bulletin of the Seismological Society of America 84, 974–1002.

Wesnousky, S., 1994. The Gutenberg-Richter or characteristic earthquake distribution, which is it?, Bulletin of the Seismological Society of America 84, 1940–1959.

Wesnousky, S. G., 2008. Displacement and geometrical characteristics of earthquake surface ruptures: Issues and implications for seismic-hazard analysis and the process of earthquake rupture, Bulletin of the Seismological Society of America 98, 4, 1609–1632.

Wiemer, S., Wyss, M., 2000. Minimum magnitude of completeness in earthquake catalogs: examples from Alaska, the Western United States, and Japan. Bulletin of the Seismological Society of America, 90, 4, 859-869.

Xu, X., Deng, Q., 1996. Nonlinear characteristics of paleoseismicity in China. Journal of Geophysical Research 101, 6209-6231.

Yetton, M., 2003. Paleoseismic trench investigation of the active trace of the Wairau section of the Apline Fault, Renwick Area, Marlborough District. Consultancy report prepared for Marlborough District Council (reference: 1490).

Yetton, M., Wells, A., 2010, Earthquake rupture history of the Alpine fault over the last 500 years, Williams et al. (eds) Geologically Active: London, Taylor and Francis Group, p. 881-891.

Zacheriasen, J., Berryman, K., Langridge, R., Prentice, C., Rymer, M., Stirling, M., Villamor, P., 2006. Timing of late Holocene surface rupture of the Wairau Fault, Marlborough. New Zealand Journal of Geology & Geophysics 49, 159-174.

Zreda, M., Noller, J., 1998. Ages of prehistoric earthquakes revealed by cosmogenic chloride-36 in a bedrock scarp at Hebgen Lake. Science 282, 1097-1099.

APPENDICES

APPENDIX 1: COMPILATION OF PALEOEARTHQUAKE TIMING, RECURRENCE AND SLIP (SINGLE-EVENT DISPLACEMENT) FOR THE FAULTS STUDIED IN THIS REPORT (SEE TABLE 2.1 FOR SUMMARY)

Name and number in first row corresponds to name and number in Table 2.1. Event timing is presented in years before 2010 with uncertainties of 2σ. Recurrence interval and mean recurrence interval uncertainties are 1σ. Uncertainties on slip are assumed to be 2σ. Mean recurrence and slip and its uncertainty (1σ) are calculated from the histograms generated by the Monte Carlo method. Where no histogram was produced for slip the mean and standard deviation were calculated from the raw paleoearthquake data and are marked by an "*" (where both approaches were used they typically produced values within 1% of each other). All timing and recurrence estimates are rounded to the nearest 10 years except where the timing of an event is known to within <10 years. Slip measurements are rounded to the nearest 10 cm. COV are rounded to two decimal places.

Eastern Awatere Fault (1)						
Event	**Event Timing (years BP 2010)**		**Recurrence Interval (years)**		**Slip (m)**	
	Value	**Uncertainty (±2σ)**	**Value**	**Uncertainty (±1σ)**	**Value**	**Uncertainty (±2σ)**
1	162				5.3	1.6
2	1090	50	928	30	5	2
3	1510	150	420	100		
4	3210	150	1700	150		
5	4360	300	1150	230		
6	5040	325	680	320		
7	5200	175	160	250		
8	6110	135	910	160		
9	6700	150	595	150		
10	8530	140	1830	150		
Mean recurrence (yrs)	930±540					
Mean Slip (m)	5.15±0.9*					
Recurrence COV	0.58					
Slip COV	Insufficient data					
Comments: Source - Benson et al., 2001; Mason et al., 2006. Timing of event 7 included but requires further testing.						

Rototipakau Fault (2)						
Event	Event Timing (years BP 2010)		Recurrence Interval (years)		Slip (m)	
	Value	Uncertainty (±2σ)	Value	Uncertainty (±1σ)	Value	Uncertainty (±2σ)
1	23					
2	360	200	340	100		
3	510	200	150	200		
4	2060	1400	1550	800		
5	4760	800	2700	1100		
6	6560	1000	1800	900		
7	7060	1000	500	1000		
8	7560	1000	500	1000		
9	10560	1000	3000	1000		
Mean recurrence (yrs)	1315±1130					
Mean Slip (m)	No data					
Recurrence COV	0.86					
Slip COV	No data					
Comments: Source - Berryman et al. 1998						

Wairau Fault (3)						
Event	Event Timing (years BP 2010)		Recurrence Interval (years)		Slip (m)	
	Value	Uncertainty (±2σ)	Value	Uncertainty (±1σ)	Value	Uncertainty (±2σ)
1	2060	300			6	1.5
2	2860	400	800	350	5	2
3	5310	350	2450	380	8	2.5
4	7860	800	2550	580	9	2.8
5	10460	400	2600	600	8	2.8
6	11310	750	850	580	11.5	2.8
7	14160	1800	2850	1280	6.5	3.6
8	17960	2300	3800	2050		
Mean recurrence (yrs)	2260±1340					
Mean Slip (m)	7.7±2.4					
Recurrence COV	0.59					
Slip COV	0.31					
Comments: Source - Zacharisen et al., 2006; Barnes & Pondard, 2010; Van Dissen & Nicol unpublished data, 2011; Nicol et al., 2011.						

Rangipo Fault (4)						
Event	Event Timing (years BP 2010)		Recurrence Interval (years)		Slip (m)	
	Value	Uncertainty (±2σ)	Value	Uncertainty (±1σ)	Value	Uncertainty (±2σ)
1	1010	850			0.1	0.2
2	2220	400	1210	200	0.14	0.2
3	3090	470	870	660	0.8	0.3
4	4860	300	1770	390	0.35	0.3
5	8510	1250	3650	780	1.2	0.3
6	10910	300	2400	780		0.3
7	12110	250	1200	280	0.4	0.3
Mean recurrence (yrs)		1890±1570				
Mean Slip (m)		0.50±0.42				
Recurrence COV		0.83				
Slip COV		0.85				
Comments: Source - Villamor et al., 2007.						

Whirinaki Fault (5)						
Event	Event Timing (years BP 2010)		Recurrence Interval (years)		Slip (m)	
	Value	Uncertainty (±2σ)	Value	Uncertainty (±1σ)	Value	Uncertainty (±2σ)
1	560	50			0.7	0.2
2	1480	300	917	150	0.5	0.2
3	3560	1800	2080	925	1.3	0.3
4	7060	1500	3500	1650	1	0.3
5	9510	50	2450	775	0.7	0.3
6	14560	900	5050	475	1.5	0.3
7	17060	1500	2500	1200	0.8	0.3
8	24060	3000	7000	2250	3	0.3
Mean recurrence (yrs)		3360±2050				
Mean Slip (m)		0.93±0.36				
Recurrence COV		0.61				
Slip COV		0.39				
Comments: Source - Canora-Catalan et al. 2008, Fitzpatrick Trench on NW Section of West Strand & Matthews Trench on SE Section of West Strand, Event 8 slip is inferred to comprise multiple events and has not been included in mean slip calculation.						

Paeroa Fault (6)						
Event	Event Timing (years BP 2010)		Recurrence Interval (years)		Slip (m)	
	Value	Uncertainty (±2σ)	Value	Uncertainty (±1σ)	Value	Uncertainty (±2σ)
1	460	140			1.7	0.2
2	1310	400	850	200	1.4	0.2
3	2000	300	690	220	1.7	0.3
4	7500	500	5500	400	1.4	0.3
5	8700	700	1200	600	2.3	0.3
6	12800	800	4100	750	3.9	0.3
7	16200	800	3400	800	0.6	0.3
Mean recurrence (yrs)	2620±1990					
Mean Slip (m)	1.8±1.0					
Recurrence COV	0.76					
Slip COV	0.56					
Comments: Source - Berryman et al., 2008, Seven trenches (Doney 1, Fraser-Pain 1, Forest 1, Forest 2, Field 1, Field 2, Field 3) along 5 km long Northern Section - 5 of 11 subparallel fault strands						

Pihama Fault (7)						
Event	Event Timing (Years BP 2010)		Recurrence Interval (years)		Slip (m)	
	Value	Uncertainty (±2σ)	Value	Uncertainty (±1σ)	Value	Uncertainty (±2σ)
1	3060	3000			1	0.3
2	6310	250	3250	1630	0.6	0.4
3	12060	1000	5750	630	1.5	0.5
4	22610	1850	10550	1430	0.9	0.2
5	27560	1000	4950	1430	0.6	0.2
6	46060	9000	18500	5000	0.8	0.2
7	67060	12500	21000	10750	0.6	0.2
Mean recurrence (yrs)	10660±8180					
Mean Slip (m)	0.86±0.34					
Recurrence COV	0.77					
Slip COV	0.40					
Comments: Source - Townsend et al. 2010; Nicol et al. unpublished data, 2011						

Cloudy Fault (8)						
Event	Event Timing (years BP 2010)		Recurrence Interval (years)		Slip (m)	
	Value	Uncertainty (±2σ)	Value	Uncertainty (±1σ)	Value	Uncertainty (±2σ)
1	1800	300			2	0.2
2	3100	600	1300	900	1	0.2
3	8700	1600	5600	2200	2.3	0.3
4	9700	1700	1000	3300	6.4	0.3
5	13200	2600	3500	4300	3.9	0.3
6	16200	3700	3000	6300	1.8	0.3
Mean recurrence (yrs)		3000±2120				
Mean Slip (m)		2.9±1.8				
Recurrence COV		0.71				
Slip COV		0.62				
Comments: Source - Pondard & Barnes 2010						

Mangatete Fault (9)						
Event	Event Timing (years BP 2010)		Recurrence Interval (years)		Slip (m)	
	Value	Uncertainty (±2σ)	Value	Uncertainty (±1σ)	Value	Uncertainty (±2σ)
1	1010	750			1	0.3
2	6560	1000	5550	880	0.5	0.3
3	11060	1500	4500	1250	1.5	0.3
4	14560	900	3500	1200	0.6	0.3
5	19360	2100	4800	1500	0.9	0.3
6	24210	2350	4450	2220	1.6	0.3
Mean recurrence (yrs)		4640±1480				
Mean Slip (m)		1.02±0.44				
Recurrence COV		0.31				
Slip COV		0.43				
Comments: Source - Nicol et al. unpublished data, 2011						

Eastern Porters Pass Fault (10)						
Event	Event Timing (years BP 2010)		Recurrence Interval (years)		Slip (m)	
	Value	Uncertainty (±2σ)	Value	Uncertainty (±1σ)	Value	Uncertainty (±2σ)
1	610	50			6	3
2	1010	150	400	100	5	2.5
3	2460	100	1450	130	7	3.5
4	5310	750	2850	430	5	2.5
5	6360	500	1050	630	7.5	3.75
6	8760	300	2400	400	7.5	3.75
Mean recurrence (yrs)		1630±960				
Mean Slip (m)		6.34±1.64				
Recurrence COV		0.59				
Slip COV		0.26				
Comments: Source - Howard et. al., 2005; Campbell unpublished data 2010						

Southern Wairarapa Fault (11)						
Event	Event Timing (years BP 2010)		Recurrence Interval (years)		Slip (m)	
	Value	Uncertainty (±2σ)	Value	Uncertainty (±1σ)	Value	Uncertainty (±2σ)
1	155				15.5	1.4
2	920	60	770	30	13.9	0.6
3	2210	100	1290	80		
4	3500	200	1290	145		
5	5090	190	1590	190		
6	6830	160	1740	170		
Mean recurrence (yrs)		1330±360				
Mean Slip (m)		16.94±3.54*				
Recurrence COV		0.27				
Slip COV		0.21				
Comments: Source – Rodgers & Little, 2006; Little et al., 2009						

Alpine Fault (12)						
Event	**Event Timing (years BP 2010)**		**Recurrence Interval (years)**		**Slip (m)**	
	Value	**Uncertainty (±2σ)**	**Value**	**Uncertainty (±1σ)**	**Value**	**Uncertainty (±2σ)**
1	184	0			8	
2	293	1	109	1	9	
3	395	5	102	6		
4	580	20	190	10		
5	780	50	200	40		
Mean recurrence (yrs)		149±47 (162±45)				
Mean Slip (m)		8.5±0.5*				
Recurrence COV		0.32				
Slip COV		Insufficient data				
Comments: Events located along the entire length of the Alpine Fault. Event 1 assigned assuming 1826 Fiordland earthquake was on Alpine Fault (Yetton and Wells, 2010). Mean recurrence in brackets omits 1826 event. Hokuri Creek recurrence from Berryman et al. (2012) (mean 329±122 years) not included in Table (see text for further discussion. Source - Wells et al., 1999; Wells & Goff, 2007; Yetton & Wells 2010						

Hope Fault (13)						
Event	**Event Timing (years BP 2010)**		**Recurrence Interval (years)**		**Slip (m)**	
	Value	**Uncertainty (±2σ)**	**Value**	**Uncertainty (±1σ)**	**Value**	**Uncertainty (±2σ)**
1	122				2	0.5
2	230	30	110	20		
3	390	40	160	20		
4	500	30	110	10		
5	630	30	130	20		
Mean recurrence (yrs)		130±30				
Mean Slip (m)		Insufficient data				
Recurrence COV		0.27				
Slip COV		Insufficient data				
Comments: Hope River segment. Source - Cowan & McGlone 1991						

Kiri Fault (14)						
Event	Event Timing (years BP (2010)		Recurrence Interval (years)		Slip (m)	
	Value	Uncertainty (±2σ)	Value	Uncertainty (±1σ)	Value	Uncertainty (±2σ)
1	990	770			1.2	0.4
2	2160	200	1170	490		
3	2580	170	420	190		
4	3060	200	480	190		
5	4560	1500	1500	850		
Mean recurrence (yrs)	910±710					
Mean Slip (m)	Insufficient data					
Recurrence COV	0.78					
Slip COV	Insufficient data					
Comments: Source – Townsend et al. 2010, Mouslopoulou et al 2012						

Lachlan Fault (15)						
Event	Event Timing (years BP 2010)		Recurrence Interval (years)		Slip (m)	
	Value	Uncertainty (±2σ)	Value	Uncertainty (±1σ)	Value	Uncertainty (±2σ)
1	610	100				
2	2070	50	1460	80		
3	3950	80	1880	70		
4	4140	80	190	80		
5	5340	80	1200	80		
Mean recurrence (yrs)	1180±620					
Mean Slip (m)	No data					
Recurrence COV	0.53					
Slip COV	No data					
Comments: Source - Berryman 1993, Barnes et al. 2002						

Ngakuru Fault (16)						
Event	Event Timing (Years BP 2010)		Recurrence Interval (years)		Slip (m)	
	Value	Uncertainty (±2σ)	Value	Uncertainty (±1σ)	Value	Uncertainty (±2σ)
1	690	300			1	0.3
2	7560	1000	6870	1300	0.75	0.3
3	10560	1000	3000	2000	2.35	0.3
4	26320	920	15760	1000	1.4	0.3
Mean recurrence (yrs)	8540±5380					
Mean Slip (m)	1.38±0.62					
Recurrence COV	0.63					
Slip COV	0.45					
Comments: Source – Nicol et al. unpublished data, 2011						

Ohariu Fault (17)						
Event	Event Timing (years BP 2010)		Recurrence Interval (years)		Slip (m)	
	Value	Uncertainty (±2σ)	Value	Uncertainty (±1σ)	Value	Uncertainty (±2σ)
1	200	60			3.7	1.3
2	1090	30	890	40		
3	2460	70	1370	48		
4	4000	800	1540	435		
5	4900	500	900	650		
Mean recurrence (yrs)	1180±460					
Mean Slip (m)	Insufficient data					
Recurrence COV	0.39					
Slip COV	Insufficient data					
Comments: Source – Heron et al. 1998; Litchfield et al. 2006, Litchfield et al., 2010						

Snowdon Fault (18)						
Event	**Event Timing (years BP 2010)**		**Recurrence Interval (years)**		**Slip (m)**	
	Value	**Uncertainty (±2σ)**	**Value**	**Uncertainty (±1σ)**	**Value**	**Uncertainty (±2σ)**
1	1010	750			0.22	0.1
2	2660	800	1650	775	0.6	0.2
3	11060	1000	8400	900	0.6	0.2
4	14560	900	3500	950	0.75	0.2
5	20060	2500	5500	1700	0.65	0.2
Mean recurrence (yrs)		4760±2710				
Mean Slip (m)		0.50±0.20				
Recurrence COV		0.57				
Slip COV		0.40				
Comments: Source – Nicol et al., 2007; Nicol et al., 2010; Nicol et al. unpublished data 2011						

Vernon Fault (19)						
Event	**Event Timing (years BP (2010)**		**Recurrence Interval (years)**		**Slip (m)**	
	Value	**Uncertainty (±2σ)**	**Value**	**Uncertainty (±1σ)**	**Value**	**Uncertainty (±2σ)**
1	3200	700			1.3	0.2
2	5200	1200	2000	600	2.6	0.2
3	9200	2500	4000	1600	0.8	0.3
4	11400	3300	2200	2900	0.4	0.3
5	15300	3500	3900	3400	1.1	0.3
Mean recurrence (yrs)		3140±1890				
Mean Slip (m)		1.24±0.76				
Recurrence COV		0.61				
Slip COV		0.62				
Comments: Source - Pondard & Barnes 2010						

Wellington Fault (20)						
Event	Event Timing (years BP (2010)		Recurrence Interval (years)		Slip (m)	
	Value	Uncertainty (±2σ)	Value	Uncertainty (±1σ)	Value	Uncertainty (±2σ)
1	270	100			5.3	0.4
2	920	70	630	85	6.2	2.2
3	2150	250	1230	180	2.8	2.7
4	3740	1220	1590	735	5.8	1.7
5	7900	550	4160	880		
Mean recurrence (yrs)	1910±1440					
Mean Slip (m)	5.03±1.53					
Recurrence COV	0.75					
Slip COV	0.30					
Comments: Hutt Valley segment of the fault. Mean and standard deviation for slip from Little et al. 2010. Source - Little et al., 2010; Langridge et al., 2009 & 2011						

Eastern Clarence Fault (21)						
Event	Event Timing (years BP (2010)		Recurrence Interval (years)		Slip (m)	
	Value	Uncertainty (±2σ)	Value	Uncertainty (±1σ)	Value	Uncertainty (±2σ)
1	1820	160			7	2
2	2560	600	740	380	7	2
3	4000	800	1440	700		0.2
4	6600	400	2600	600		0.2
Mean recurrence (yrs)	1590±920					
Mean Slip (m)	7±2					
Recurrence COV	0.58					
Slip COV	Insufficient data					
Comments: Source - Van Dissen & Nicol 2009						

Ihaia Fault (22)						
Event	Event Timing (years BP 2010)		Recurrence Interval (years)		Slip (m)	
	Value	Uncertainty (±2σ)	Value	Uncertainty (±1σ)	Value	Uncertainty (±2σ)
1	410	200			1.2	0.4
2	3060	200	2650	200		
3	4560	500	1500	350		
4	5860	500	1300	500		
Mean recurrence (yrs)	1820±680					
Mean Slip (m)	Insufficient data					
Recurrence COV	0.37					
Slip COV	Insufficient data					
Comments: Source – Mouslopoulou et al. unpublished data 2011; Mouslopoulou et al. 2012						

Matata Fault (23)						
Event	Event Timing (years BP 2010)		Recurrence Interval (years)		Slip (m)	
	Value	Uncertainty (±2σ)	Value	Uncertainty (±1σ)	Value	Uncertainty (±2σ)
1	270	50				
2	510	200	240	120		
3	1690	230	1180	210		
4	2560	800	870	510		
Mean recurrence (yrs)	790±490					
Mean Slip (m)	No data					
Recurrence COV	0.62					
Slip COV	No data					
Comments: Source - Ota et al., 1988; Begg and Mouslopoulou 2010						

Oaonui Fault (24)						
Event	Event Timing (years BP 2010)		Recurrence Interval (years)		Slip (m)	
	Value	Uncertainty (±2σ)	Value	Uncertainty (±1σ)	Value	Uncertainty (±2σ)
1	990	720			0.6	0.1
2	10160	1900	9180	1310	0.5	0.2
3	19560	2000	9400	1950	0.5	0.1
4	23860	1200	4300	1600	0.4	0.1
Mean recurrence (yrs)	7620±2770					
Mean Slip (m)	0.5±0.1					
Recurrence COV	0.36					
Slip COV	0.2					
Comments: Source - Townsend et al., 2010; Mouslopoulou et al. unpublished data, 2011						

Rotohauhau Fault (25)						
Event	Event Timing (years BP 2010)		Recurrence Interval (years)		Slip (m)	
	Value	Uncertainty (±2σ)	Value	Uncertainty (±1σ)	Value	Uncertainty (±2σ)
1	1010	750			0.5	0.2
2	2660	800	1650	780	1	0.3
3	14560	900	11900	850	0.9	0.3
4	16360	900	1800	900	0.9	0.3
Mean recurrence (yrs)	5100±4870					
Mean Slip (m)	0.83±0.24					
Recurrence COV	0.95					
Slip COV	0.29					
Comments: Source - Nicol et al. 2010, Nicol et al. unpublished data 2011.						

APPENDIX 2: RECURRENCE INTERVAL HISTOGRAMS FOR FAULTS IN TABLE 2.1 WITH 4-6 RECORDED EARTHQUAKES. HISTOGRAMS GENERATED USING THE MONTE CARLO METHOD DESCRIBED IN THE MAIN BODY OF THE TEXT. SEE TABLE 2.1 FOR SUMMARY OF PALEOEARTHQUAKE HISTORIES FOR EACH FAULT

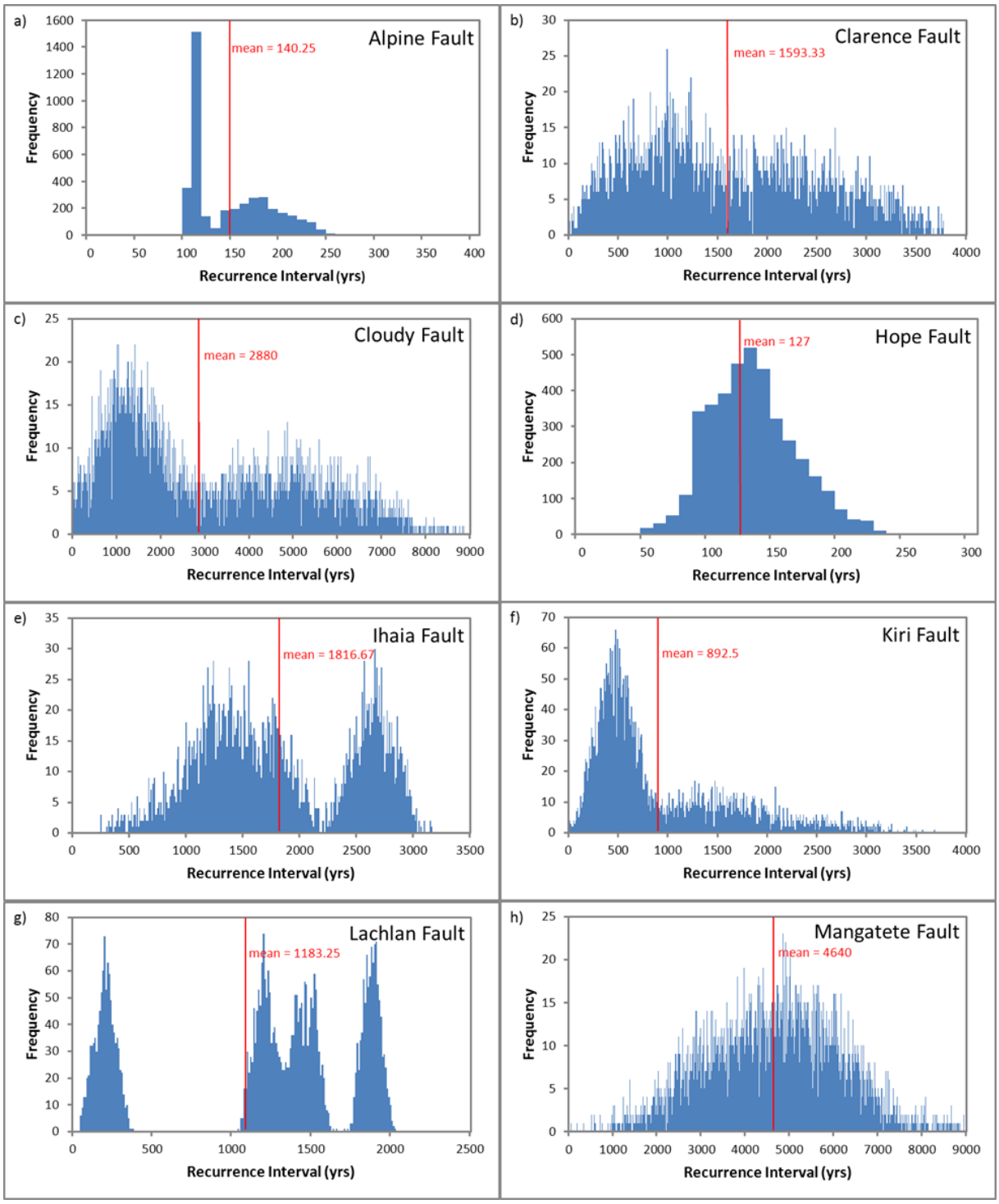

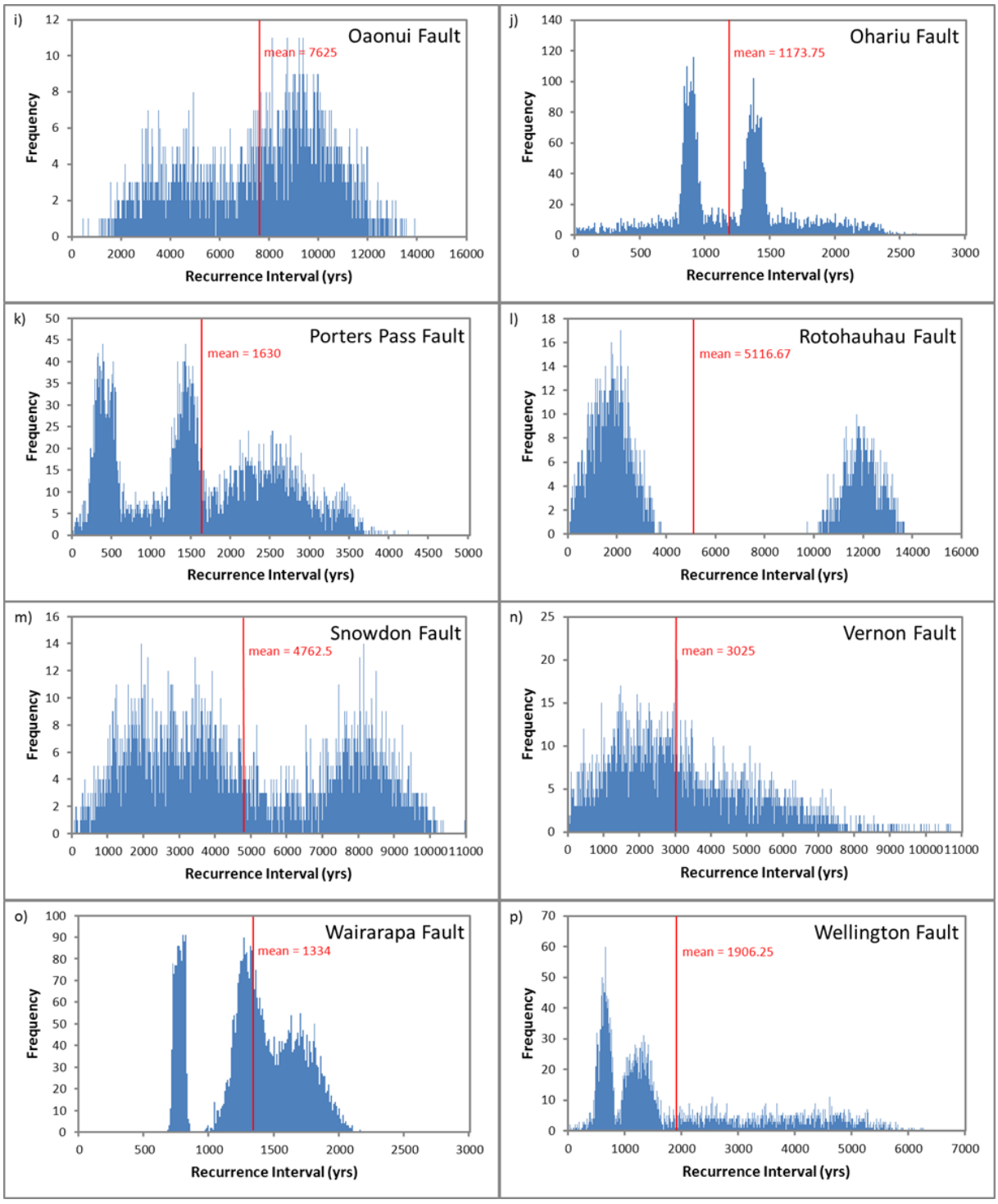
i)
Oaonui Fault
mean = 7625
Frequency
Recurrence Interval (yrs)
j)
Ohariu Fault
mean = 1173.75
Frequency
Recurrence Interval (yrs)
k)
Porters Pass Fault
mean = 1630
Frequency
Recurrence Interval (yrs)
l)
Rotohauhau Fault
mean = 5116.67
Frequency
Recurrence Interval (yrs)
m)
Snowdon Fault
mean = 4762.5
Frequency
Recurrence Interval (yrs)
n)
Vernon Fault
mean = 3025
Frequency
Recurrence Interval (yrs)
o)
Wairarapa Fault
mean = 1334
Frequency
Recurrence Interval (yrs)
p)
Wellington Fault
mean = 1906.25
Frequency
Recurrence Interval (yrs)

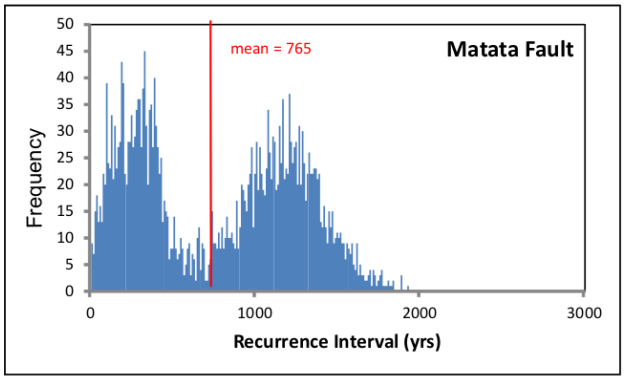
Matata Fault
mean = 765
Frequency
Recurrence Interval (yrs)

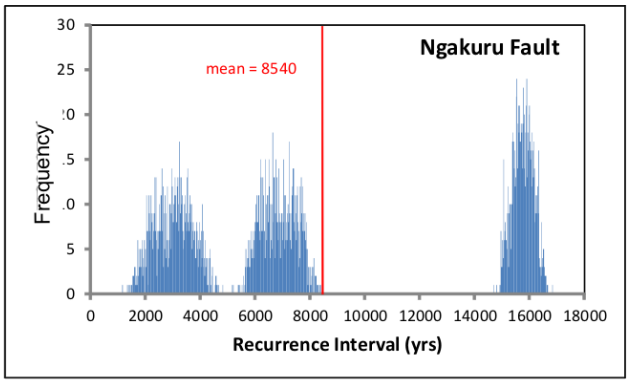
Ngakuru Fault
mean = 8540
Frequency
Recurrence Interval (yrs)

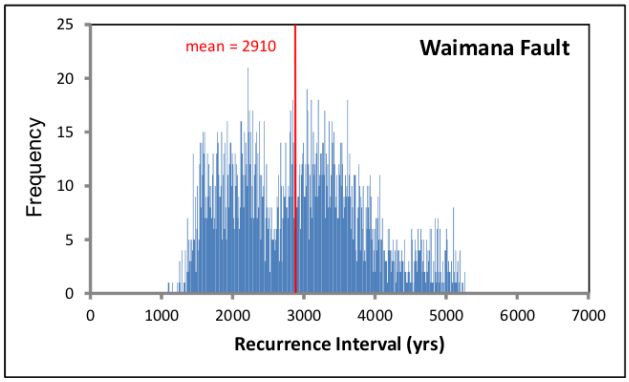
Waimana Fault
mean = 2910
Frequency
Recurrence Interval (yrs)

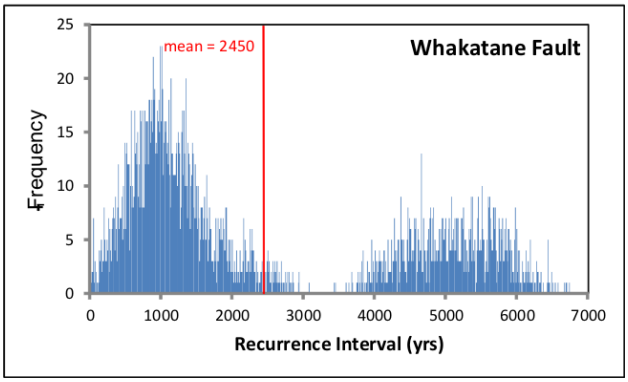
Whakatane Fault
mean = 2450
Frequency
Recurrence Interval (yrs)

www.gns.cri.nz

Principal Location

1 Fairway Drive
Avalon
PO Box 30368
Lower Hutt
New Zealand
T +64-4-570 1444
F +64-4-570 4600

Other Locations

Dunedin Research Centre
764 Cumberland Street
Private Bag 1930
Dunedin
New Zealand
T +64-3-477 4050
F +64-3-477 5232

Wairakei Research Centre
114 Karetoto Road
Wairakei
Private Bag 2000, Taupo
New Zealand
T +64-7-374 8211
F +64-7-374 8199

National Isotope Centre
30 Gracefield Road
PO Box 31312
Lower Hutt
New Zealand
T +64-4-570 1444
F +64-4-570 4657